applied sciences

MDPI

Article

Effective Equations for the Optimum Seismic Gap Preventing Earthquake-Induced Pounding between Adjacent Buildings Founded on Different Soil Types

Mahmoud Miari * and Robert Jankowski

Faculty of Civil and Environmental Engineering, Gdańsk University of Technology, Ul. Narutowicza 11/12, 80-233 Gdańsk, Poland; jankowr@pg.edu.pl

* Correspondence: mahmoud-miari@hotmail.com or mahmoud.miari@pg.edu.pl

Abstract: The best approach to avoid collisions between adjacent structures during earthquakes is to provide sufficient spacing between them. However, the existing formulas for calculating the optimum seismic gap preventing pounding were found to provide inaccurate results upon the consideration of different soil types. The aim of this paper is to propose new equations for the evaluation of the sufficient in-between separation gap for buildings founded on different soil conditions. The double-difference formula has been taken into account in this study. The seismic gap depends on the correlation factor and on the top displacements of adjacent buildings. The correlation factor depends on the ratio of the periods of adjacent buildings (smaller period to larger period). The modification of the correlation factor has been introduced for buildings founded on five different soil types. Five soil types were taken into account in this study, as defined in the ASCE 7-10 code, i.e., hard rock, rock, very dense soil and soft rock, stiff soil, and soft clay soil. The normalized root mean square errors have been calculated for the proposed equations. The results of the study indicate that the error ranges between 2% and 14%, confirming the accuracy of the approach. Therefore, the proposed equations can be effectively used for the determination of the optimum seismic gap preventing earthquake-induced pounding between buildings founded on different soil types.

Keywords: structural pounding; buildings; earthquakes; optimum seismic gap; soil types; least square method

Citation: Miari, M.; Jankowski, R. Effective Equations for the Optimum Seismic Gap Preventing Earthquake-Induced Pounding between Adjacent Buildings Founded on Different Soil Types. *Appl. Sci.* **2023**, *13*, 9741. https://doi.org/10.3390/app13179741

Academic Editor: José A. Peláez

Received: 9 August 2023
Revised: 21 August 2023
Accepted: 23 August 2023
Published: 28 August 2023

1. Introduction

One of the most dangerous phenomena occurring during earthquakes is related to the earthquake-induced structural pounding, which may have a significant effect on the response of colliding buildings [1–4] as well as on the damage state [5]. Structural pounding has been observed in different earthquakes. For instance, in the Mexico earthquake (1985), 40% of the damaged buildings experienced pounding, and, in 15% of the severely damaged or collapsed structures, pounding was found [6], where, in 20–30% of them, collisions could be the major reason of damage [7]. Indeed, in the Loma Prieta earthquake, pounding was experienced in 200 out of 500 surveyed buildings [8]. Moreover, collisions were also observed in recent earthquakes, such as in Lorca (Spain 2001) [9], Wenchuan (Sichuan Province in China in 2008) [10], Christchurch (New Zealand 2010) [11,12], Christchurch (2011) [13,14], and Gorkha (Nepal 2015) [15–20].

The research on earthquake-induced structural pounding, as well as on different methods to prevent it, has been conducted for more than three decades (see, for example, [21,22]). Pounding leads to the amplification in the peak interstorey drift (IDR), residual IDR, floor peak accelerations, shear forces, and impact forces, while the displacements may increase or decrease [23–27]. This amplification is significant in the direction of pounding and insignificant in the other directions [28]. The degree of amplification depends on the dynamic properties of colliding buildings, and this amplification is more significant when there

is a major difference in the dynamic properties of colliding structures [1,29]. Also, the impact force depends on the earthquake characteristics as well as on the relation between the natural frequencies of the colliding buildings [30]. Indeed, in some studies [31,32], pounding was found to have a greater effect on the response of the flexible structure, as compared to the stiff one, and it was found to have a greater effect on the response of the stiff structure, as compared to the flexible one, in other studies [33]. Furthermore, using the Monte Carlo simulations based on Sobol's method, Crozet et al. [34,35] found that the frequency ratio had the largest influence on the maximum impact force and ductility demands while the frequency and mass ratios had the largest influence on the impact impulse (mass ratio is predominant for low frequency range).

The in-between seismic gap has a significant influence on the response of colliding buildings. However, increasing the seismic gap does not necessarily lead to the reduction in the effects of pounding, unless it is large enough to totally eliminate structural collisions [28,33]. Several formulas have been suggested to evaluate the optimum seismic gap preventing pounding, i.e., the absolute sum (ABS) formula (Equation (1)) [36], square root of the sum of the squares (SRSS) formula (Equation (2)) [29], double-difference (DDC) formula (Equations (3) and (4)) [37], Australian Code formula (Equation (5)) [38], and Naderpour et al. formula (Equations (3) and (6)) [39].

$$S = U_1 + U_2 \tag{1}$$

$$S = \sqrt{{U_1}^2 + {U_2}^2} \tag{2}$$

$$S = \sqrt{{U_1}^2 + {U_2}^2 - 2\rho U_1 U_2} \tag{3}$$

$$\rho = \frac{8\left(\sqrt{\xi_1 \xi_2}\right)\left(\xi_2 + \xi_1 \frac{T2}{T1}\right)\left(\frac{T2}{T1}\right)^{1.5}}{\left[1 - \left(\frac{T2}{T1}\right)^2\right]^2 + 4\xi_1\xi_2\left[1 + \left(\frac{T2}{T1}\right)^2\right]\left(\frac{T2}{T1}\right) + 4\left({\xi_1}^2 + {\xi_2}^2\right)\left(\frac{T2}{T1}\right)^2} \tag{4}$$

$$S = 0.01 H_{max} \tag{5}$$

$$\rho = \left(\frac{T_2}{T_1}\right) - 10.5(T_2 - T_1) \tag{6}$$

where S is the sufficient seismic separation gap, U_1, ξ_1, and T_1 are the design displacement, damping ratio, and natural period for the first building, and U_2, ξ_2, and T_2 are the design displacement, damping ratio, and natural period for the second building ($T_1 < T_2$), respectively; ρ stands for the correlation factor and H_{max} is the height of the taller structure. The DDC formula involves the evaluation of the seismic gap based on the maximum displacements of both buildings and the correlation factor. The correlation factor represents the uncertainties in earthquake-induced structural pounding. The accurate estimation of the seismic gap between adjacent buildings based on the DDC formula requires a proper consideration of the uncertainties involved in the pounding phenomena. The correlation factor depends on the natural periods of adjacent buildings, which represent the dynamic properties of the vibrating structures, including the mass and the stiffness. Most of the studies concerning earthquake-induced structural pounding ignored the soil type and the soil–structure interaction (SSI). However, the SSI and the soil type have a significant influence on the response of vibrating buildings due to the fact that the flexibility induced by soil decreases the stiffness of the colliding buildings [40]. Furthermore, in the case of braced frames, taking into account fixed base buildings is considered conservative and it is not necessary to consider SSI. However, in the case of unbraced frames resting on soft soil, the consideration of the SSI is necessary. This refers to several factors, including the fact that

the SSI has a significant influence on the interstorey drifts and the lateral deflections [41]. Moreover, through the comparison of the responses of unbraced frames resting on soft soil considering fixed base buildings as well as considering SSI, it can be concluded that the SSI significantly increases the interstorey drifts and decreases the base shear [42]. Indeed, the necessity of considering SSI increases as the shear wave velocity and shear modulus of the soil decrease [43–45]. Also, considering nonlinearity is important in SSI problems to obtain results with acceptable accuracy [46]. Because considering SSI can change the structural dominant frequency and lead to a mistuned mass damper, Wang et al. [47–49] developed advanced versions of mistuned mass dampers to adjust to the effects of considering SSI, to control human-induced vibrations, as well as to control the vibrations of base-isolated buildings. It is worth noting that several methods have been proposed for the numerical evaluation of the response of vibrating buildings taking into account SSI [45,50,51]. Also, several methods have been proposed for the experimental evaluation of the response of vibrating buildings taking into account SSI using the shaking table tests (see [52,53], for example). More details were reported in the literature, providing an in-depth description of considering SSI experimentally, describing the necessary procedure and equipment for the consideration of the SSI, including creating the physical model [54] and the soil mixture [55]. Furthermore, previous studies confirm that pounding is significant in the case of SSI as well as in the case of soil–pile–structure interaction [56,57]. Several contradictory results about the effects of the SSI on the response of colliding buildings have been reported in the literature. It was found that pounding with SSI leads to the increase in the displacements, shear forces, and impact forces in some studies (see [56,58–63], for example). However, in some other studies (see [64,65], for example), it was found that pounding with SSI leads to the decrease in the displacements, shear forces, and impact forces. The contradictory results referred to several factors that were overlooked in these studies, such as the soil type, since the effects of the soil type have been ignored in some studies and the fact that these studies considered different soil types.

Recently, Miari et al. [66–68] studied the effect of the soil type on the response of buildings experiencing floor-to-floor pounding during earthquakes. Five soil types have been considered in the investigation, as defined in the ASCE 7-10 code [69], i.e., hard rock, rock, very dense soil and soft rock, stiff soil, and soft clay soil. The results of the study show that pounding is more significant for the buildings founded on the soft clay soil than for buildings founded on stiff soil, than for buildings founded on very dense soil and soft rock, and finally for buildings founded on the rock and hard rock. Indeed, Miari et al. [70] studied the effects of the soil type on the response of buildings experiencing floor-to-column pounding where special attention has been paid to the shear demands of the impacted column (the column experiencing the hit from the top slab of the shorter building). The same five soil types have been taken into account. It was found that the shear demands of the impacted column significantly increase due to collisions. Also, it was found that the impacted column experiences higher shear demands for buildings founded on the soft clay soil than for buildings founded on the stiff soil, than for buildings founded on very dense soil and soft rock, and finally for buildings founded on the rock and hard rock. Moreover, Miari et al. [71] studied experimentally (using the shaking table tests) the effects of the soil type on the response of colliding buildings. Two steel-storey buildings with different dynamic properties have been considered in the case of pounding as well as the no-pounding case. Four seismic gaps and five earthquakes have been considered in the study. The same five soil types have been taken into account. The results of this study reveal that the soil type has a significant effect on the response of buildings in the case of pounding as well as in the no-pounding case. However, the soil type effect is more significant in the case of pounding than the no-pounding case. Furthermore, Miari et al. [72–74] investigated the accuracy of five different formulas (ABS, SRSS, DDC, Australian Code, and Naderpour et al. formula; see Equations (1)–(6)) in evaluating the seismic gap upon the consideration of different soil conditions. The same five soil types have been taken into account. It was found that the seismic gap has a significant influence on the response of colliding buildings.

For all soil types, larger gaps do not necessarily lead to lower responses unless it is large enough to eliminate collisions at all (this finding was also emphasized by other works reported in the literature (see [28,33,71,75], for example)). The results of this study also show that all five formulas provide poor estimates when considering different soil types. The ABS and the Naderpour et al. formulas were found to be always conservative, but they overestimated the minimum gap. Moreover, the DDC and Australian Code formulas provided overestimate, accurate, and underestimate results, and the SRSS formula provided both accurate and overestimated results. Similar findings were reported concerning the Australian Code formula (Equation (5)) as it was found that it provides accurate results only in the case of the far-field earthquakes considering the in-between gap equal to 1% of the height of the taller building and not related to the height of the shorter building (see [76] for details). In the case of near-field earthquakes, or in the case when the gap was considered as equal to 1% of the height of the shorter building, the Australian Code formula (Equation (5) provides inaccurate results and underestimates the gap [76].

The aforementioned literature review illustrates that the soil types may have a significant effect on the response of colliding buildings under seismic excitation. Indeed, the currently used formulas for the evaluation of the seismic gap show the discrepancy between providing accurate, underestimate, and overestimate results upon the consideration of different types of soil. Thus, it is necessary to develop new accurate equations for the separation gap that are capable of eliminating collisions as well as taking the soil type into account. Therefore, the aim of this study is to propose new effective equations for the evaluation of the optimum seismic gap by introducing the modification of the correlation factor (see Equation (4)) for different soil types defined in the ASCE 7-10 code [69], i.e., for hard rock, rock, very dense soil and soft rock, stiff soil, and soft clay soil. By designing the buildings and providing separation between them based on the proposed equations, no collisions will occur between them, which means that providing spacing based on the proposed equations will provide more safety to the vibrating buildings during earthquakes.

2. Proposed Equations

In the process of modification of the correlation factor, 1260 pounding cases have been taken into account. In the study, 60 three-dimensional numerical models of concrete buildings have been considered. Table 1 presents the number of storeys, natural period, and frequency for each building. It should be noted that the natural period has been evaluated in the direction of possible pounding. Among these 60 numerical models, 1260 pounding cases have been considered. Table A1 in Appendix A presents a detailed description of these 1260 pounding cases, including the colliding buildings of every case as well as the period ratio between them. To generalize the proposed equations, the authors intended to consider multiple cases with varied situations and scenarios. The authors considered low-rise, mid-rise, and high-rise buildings (from 1-storey buildings up to 20-storey buildings). The torsional pounding was taken into account as well. All the cases have been studied considering five earthquake excitations. Considering the combination of all these factors has led to the generalizability of the proposed equations. These cases have concerned collisions between concrete buildings with different dynamic properties (see details in [66,67,72]), including different number of storeys (ranging from 1 storey up to 20 storeys). Among these buildings, 20 buildings have identical inertia in both directions x and y (ranging from 1 storey up to 20 storeys), 20 buildings have higher inertia in the x-direction (ranging from 1 storey up to 20 storeys), and 20 buildings have higher inertia in the y-direction (ranging from 1 storey up to 20 storeys). Figure 1 presents the plan views of the considered models. These buildings are reinforced concrete structures with a storey height of 3 m and with different lengths and widths. The shortest buildings were 3 m (one storey) and the highest buildings were 60 m (20 storeys). All the storey cases in between have been considered (buildings with 2 storeys, 3 storeys, 4 storeys, 5 storeys, up to 20 storey buildings). The properties of the material used in the models in this study are as follows: concrete with the compressive strength of 35 Mpa and the modulus of elasticity of 27.8 Gpa, steel (grade 60)

with the yield strength of 420 Mpa and the modulus of elasticity of 200 Gpa. Indeed, the live load was taken to be equal to 4 kN/m^2 and the superimposed dead load was taken to be equal to 2 kN/m^2. These values were taken considering the frequent use of such materials in construction sites. However, it should be underlined that they will not affect the accuracy of the proposed equations since the authors considered a wide range of natural structural periods, which is considered to be the main factor influencing the earthquake-induced structural pounding. Moreover, the buildings were designed to satisfy the minimum reinforcement requirements based on the ACI code (American Concrete Institute). The ACI code (in Section 10.9.1) states that the reinforcement ratio should be between 1% and 8% of the concrete area. In this study, the reinforcement ratio in the columns has been taken as equal to 1% to ensure both optimum and economic design. Also, the columns and beams were defined as frame elements, while slabs were modelled as shell elements. In this study, the frame element uses a general three-dimensional beam–column formulation that involves the effects of biaxial bending, torsion, axial deformation, and biaxial shear deformations (see [77] for details). Several damping ratios have been considered in this study so that the proposed equations will be valid for all ranges of damping ratios. All the buildings considered in this study have been modelled and designed solely for this study. The criteria of modelling have been verified using the results of shaking table experimental study [71]. For each pounding scenario, the displacement time histories for the level of possible contact (the level of the top storey of the shorter building) have been firstly obtained for both buildings vibrating independently under the specified ground motion. Then, the spacing required to avoid collisions has been calculated using Equation (7). In the next step, the peak displacements U_1 and U_2 have also been obtained for each building vibrating separately from the time history analyses. In this study, the DDC formula has been used (Equation (3)). The value of the correlation factor ρ has been calculated based on Equation (8) (obtained from re-arranging of Equation (3)). This procedure has been performed for 1260 pounding cases for buildings exposed to 5 different earthquakes and founded on 5 different soil types.

$$S = max\,|\,U_2{}^*(t) - U_1(t)\,| \tag{7}$$

$$\rho = \frac{U_1{}^2 + U_2{}^2 - S^2}{2U_1U_2} \tag{8}$$

where $U_1(t)$ is the displacement time history of the shorter building at the top storey and $U_2{}^*(t)$ is the displacement time history of the taller building at the storey corresponding to the top storey of the shorter building; e.g., if pounding occurs between 4- and 6-storey buildings, $U_1(t)$ and $U_2{}^*(t)$ concern the 4th storey of these two buildings, respectively.

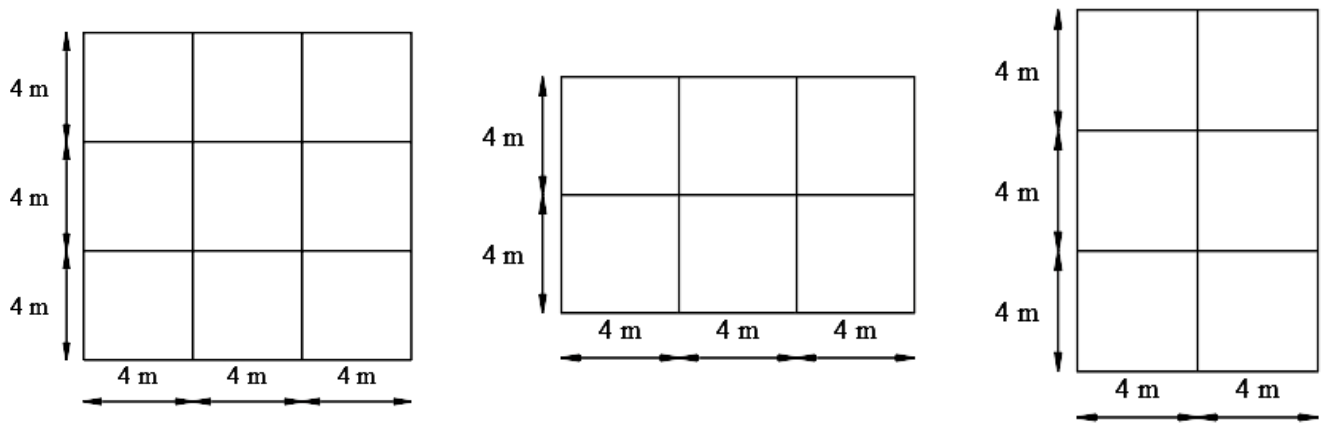

Figure 1. Plan views of the considered models.

Table 1. Dynamic properties of the considered buildings.

Building Number	Number of Storeys	Period (s)	Frequency (Hz)	Building Number	Number of Storeys	Period (s)	Frequency (Hz)
1	1	0.20	4.902	31	11	1.979	0.505
2	2	0.372	2.688	32	12	2.171	0.461
3	3	0.549	1.821	33	13	2.368	0.422
4	4	0.729	1.372	34	14	2.567	0.390
5	5	0.91	1.099	35	15	2.771	0.361
6	6	1.094	0.914	36	16	2.979	0.336
7	7	1.279	0.782	37	17	3.191	0.313
8	8	1.467	0.682	38	18	3.407	0.294
9	9	1.658	0.603	39	19	3.628	0.276
10	10	1.851	0.540	40	20	3.853	0.260
11	11	2.048	0.488	41	1	0.197	5.076
12	12	2.247	0.445	42	2	0.363	2.755
13	13	2.45	0.408	43	3	0.538	1.859
14	14	2.657	0.376	44	4	0.717	1.395
15	15	2.868	0.349	45	5	0.898	1.114
16	16	3.084	0.324	46	6	1.082	0.924
17	17	3.303	0.303	47	7	1.27	0.787
18	18	3.528	0.283	48	8	1.461	0.684
19	19	3.757	0.266	49	9	1.657	0.604
20	20	3.991	0.251	50	10	1.857	0.539
21	1	0.195	5.128	51	11	2.062	0.485
22	2	0.358	2.793	52	12	2.272	0.440
23	3	0.529	1.890	53	13	2.489	0.402
24	4	0.703	1.422	54	14	2.711	0.369
25	5	0.879	1.138	55	15	2.94	0.340
26	6	1.056	0.947	56	16	3.176	0.315
27	7	1.236	0.809	57	17	3.42	0.292
28	8	1.418	0.705	58	18	3.671	0.272
29	9	1.602	0.624	59	19	3.929	0.255
30	10	1.789	0.559	60	20	4.196	0.238

For instance, in the case of pounding between the 10-storey and 12-storey buildings (10–12 pounding scenario), the structures have been firstly studied when they vibrate independently. The displacement time histories of both buildings at the possible contact level (the level of the top storey of the shorter building, i.e., the level of 10th storey) have been obtained. In 10–12 pounding scenario, the $U_1(t)$ and $U_2{}^*(t)$ correspond to the displacement time histories at the 10th storey of the 10-storey and 12-storey building, respectively. In the next step, using Equation (7), the spacing required to avoid collisions between them has been calculated. Then, U_1 and U_2, corresponding to the peak displacement of the 10-storey and the 12-storey buildings, respectively, have been determined. After calculating the values of U_1 and U_2, as well as the spacing S, the calculation of the correlation factor has been conducted using Equation (8).

Most seismic codes require a number of 2 to 4 independent ground motion simulations so as to obtain the average responses (see [78] for details). Therefore, five ground motions have been taken into account in this study (see Table 2) downloaded from the PEER website [79]. These ground motions are ground surface records. The authors have intentionally adopted different ground motions with different PGAs and frequency content to obtain insight into the issue of how different PGAs and frequency content may contribute to the dynamic response of colliding buildings. Also, different ground motions with significantly different PGAs have been considered to ensure that the proposed equations will be valid for large range of PGAs and not limited to a specific range of PGAs.

Table 2. Earthquake records used in the study.

Earthquake	Magnitude	PGA (g)	Station	Year
Kobe	6.9	0.27577	Kobe University	1995
Parkfield	6.19	0.01175	San Luis Obispo	1966
San Fernando	6.61	0.02576	2516 Via Tejon PV	1971
Loma Prieta	6.93	0.07871	APEEL 3E Hayward CSUH	1989
Imperial Valley	6.53	0.28726	Agrarias	1979

PGA—peak ground acceleration.

The correlation factor has been calculated for each of the 1260 cases under these five ground motions and then the average value has been determined. The analysis has been performed using ETABS software v.18 [80]. Then, the correlation factor has been plotted as a function of the ratio of the natural periods of both buildings T_1/T_2 ($T_1 < T_2$). The ratio of the natural periods has been taken into account since it is the primary factor affecting the earthquake-induced structural pounding [81]. Then, the curve defined by the proposed equation has been fitted into the data set of actual values using the method of least squares. The difference between the actual results and the results based on the proposed equation has been assessed by calculating the normalized root mean square (RMS) error presented in Equation (9) (see [82]):

$$\mathrm{RMS} = \frac{\sqrt{\sum_{i=1}^{NV} \left(H_i - \overline{H}_i\right)^2}}{\sqrt{\sum_{i=1}^{NV} H_i^2}} \times 100\% \quad (9)$$

where H_i, $\overline{H}_i$ are the actual value and the value obtained by using the proposed equation, respectively, and NV denotes the number of values in the data set. Several techniques have been followed for fitting the curves, including equations with different types: polynomial, power, linear, logarithmic, and exponential. The chosen equation is the one that leads to the lowest percentage of error that is reported in the paper. The whole procedure has been performed for five soil types, A, B, C, D, and E, defined in the ASCE 7-10 code [69] (see Table 3).

Table 3. Definition of the site classes.

Site Class Description	Site Class Definition
A	Hard rock
B	Rock
C	Very dense soil and soft rock
D	Stiff soil
E	Soft clay soil

The soil type/site class has been considered by defining the response spectrum in ETABS software, and then by matching the earthquake records (defined in Table 2) with the target response spectrum. In the definition of the response spectrum, several parameters are required to be defined, which are the site class and the site properties. In this article, the value of S_s (mapped risk-targeted maximum considered earthquake spectral response acceleration parameter at short period) has been considered to be equal to 1.25, the value of S_1 (mapped risk-targeted maximum considered earthquake spectral response acceleration parameter at 1 s period) has been considered to be equal to 0.5, and the value of T_L (long transition long period) has been taken as equal to 8 s (see [66,67] for details). These values have been taken into account based on the studies conducted by Miari and Jankowski [66,67], involving extensive analysis on several scaling parameters, with the conclusion that these values lead to the highest and most significant responses. After defining these parameters, the response spectrum has been defined and the five ground motions have been scaled to the target response spectrum. The structural response has been obtained by applying the fast nonlinear analysis (FNA) method developed by Ibrahimbegovic and Wilson [83]. Jaradat and Far [84] conducted a pilot test using the direct integration, by Newmark (1959) and FNA methods. The test was conducted for the top floor relative displacement time histories for the no-pounding case. The results revealed a very good agreement between the two methods. Because of that, and considering that the FNA method consumes much less time unlike the Newmark method (which requires long period of time), the FNA method has been used in this study. In this method, the nonlinearity is considered for the gap and support elements while the linearity is considered for other elements. The dynamic equilibrium equation of the vibrating structure based on this method is shown in Equation (10).

$$K_L\, u(t) + C\, \dot{u}(t) + M\, \ddot{u}(t) + r_N(t) = -M\ddot{u}_g(t) \tag{10}$$

where K_L is the stiffness matrix for the linear elastic elements (all elements except for the gap and support elements); C is the proportional damping matrix; M is the diagonal mass matrix; $r_N(t)$ is the vector of forces from the nonlinear degrees of freedom (gap and support elements); $u(t)$, $\dot{u}(t)$, and $\ddot{u}(t)$ are vectors of the relative displacements, velocities, and accelerations with respect to the ground; and $\ddot{u}_g(t)$ is the vector of ground motion accelerations. In this study, as no gap elements have been used, the nonlinearity has been considered only for the support elements. Also, $r_N(t)$ in Equation (10) is the vector of forces from the nonlinear degrees of freedom for the support elements. A time step of 0.001 s has been used in this study since it is considered to be small enough to satisfy the conditions of numerical stability and accuracy during collisions between adjacent buildings.

It should be highlighted at the end that all the buildings considered in this study are concrete buildings and the cases involve floor-to-floor pounding in both symmetric and torsional pounding. Steel and timber buildings were not considered in this study. Therefore, the proposed equations are valid for all kinds of concrete buildings that respond in the linear elastic range: in the cases of symmetric and torsional pounding and for all ranges of stiffnesses, masses, and damping ratios.

2.1. Soil Type A

In this section, the proposed equation for the correlation factor when the colliding buildings are founded on soil type A is presented. Figure 2 presents the plot of the correlation factor when the colliding buildings are founded on soil type A versus T_1/T_2. It can be seen that the plot is a piecewise function, and it is composed of two different functions. It can also be noticed that the correlation factor follows two different trends depending on whether $T_1 \leq 0.2$ s or $T_1 > 0.2$ s (see Figure 2). Therefore, the proposed equation for the correlation factor when the colliding buildings are founded on soil type A is composed of two equations depending on whether $T_1 \leq 0.2$ s or $T_1 > 0.2$ s (see Equation (11)). Figure 3 shows a comparison between the proposed equation (Equation (11)) and the actual values of the correlation factor obtained for different cases. Using Equation (9), the RMS error has been calculated as equal to 2.94% for $T_1 \leq 0.2$ s and 12.92% for $T_1 > 0.2$ s.

$$\rho = \begin{cases} \left(\frac{T_1}{T_2}\right)^{-1.117}, & T_1 \leq 0.2 \text{ s} \\ 57.343\left(\frac{T_1}{T_2}\right)^4 - 147.46\left(\frac{T_1}{T_2}\right)^3 + 141.74\left(\frac{T_1}{T_2}\right)^2 - 61.171\left(\frac{T_1}{T_2}\right) + 10.548, & T_1 > 0.2 \text{ s} \end{cases} \quad (11)$$

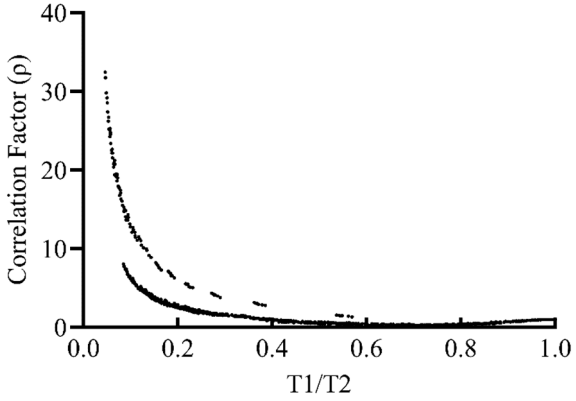

Figure 2. The correlation factor when the colliding buildings are founded on soil type A versus T_1/T_2. Both lines correspond to the same thing (correlation factor). The graph of the correlation factor is not continuous.

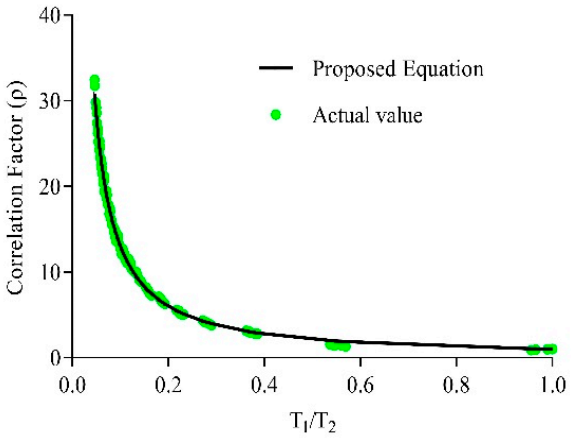

(**a**) $T_1 \leq 0.2$ s

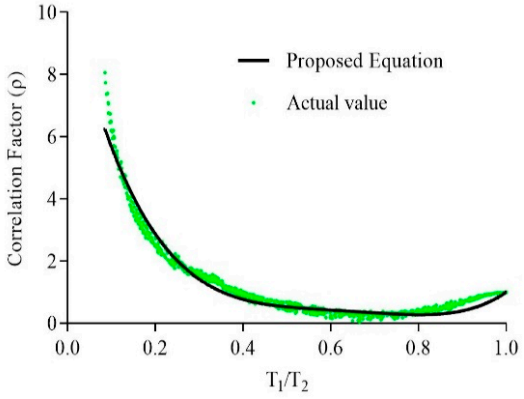

(**b**) $T_1 > 0.2$ s

Figure 3. Comparison between the actual trend and the proposed equation for the correlation factor when the colliding buildings are founded on soil type A.

2.2. Soil Type B

In this section, the proposed equation for the correlation factor when the colliding buildings are founded on soil type B is presented. Figure 4 presents the plot of the correlation factor when the colliding buildings are founded on soil type B versus T_1/T_2. It can be seen that the plot is a piecewise function, and it is composed of two different functions. It can also be noticed that the correlation factor follows two different trends depending on whether $T_1 \leq 0.2$ s or $T_1 > 0.2$ s (see Figure 4). Therefore, the proposed equation for the correlation factor when the colliding buildings are founded on soil type B is composed of two equations depending on whether $T_1 \leq 0.2$ s or $T_1 > 0.2$ s. After fitting the curves, it has been found that the equation for the correlation factor, when the colliding buildings are founded on soil type B, is the same equation for the correlation factor when the colliding buildings are founded on soil type A (see Equation (11)). Figure 5 shows a comparison between the proposed equation (Equation (11)) and the actual values of the correlation factor obtained for different cases. Using Equation (9), the RMS error has been calculated as equal to 3.00% for $T_1 \leq 0.2$ s and 13.17% for $T_1 > 0.2$ s.

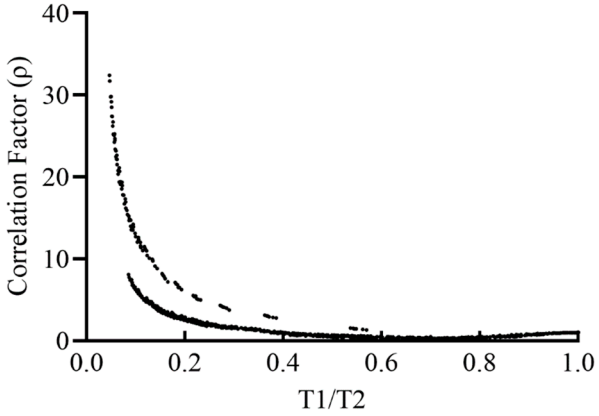

Figure 4. The correlation factor when the colliding buildings are founded on soil type B versus T_1/T_2. Both lines correspond to the same thing (correlation factor). The graph of the correlation factor is not continuous.

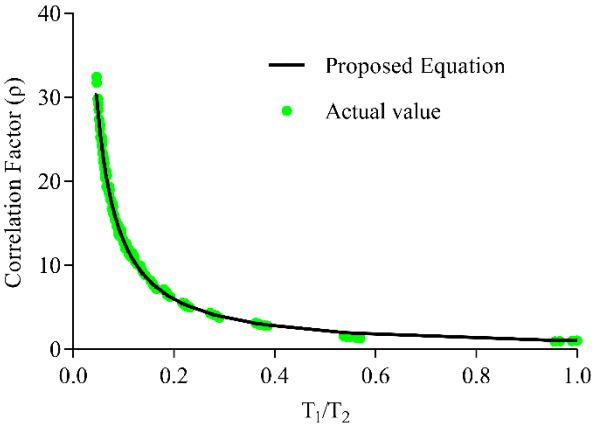

(**a**) $T_1 \leq 0.2$ s

Figure 5. *Cont.*

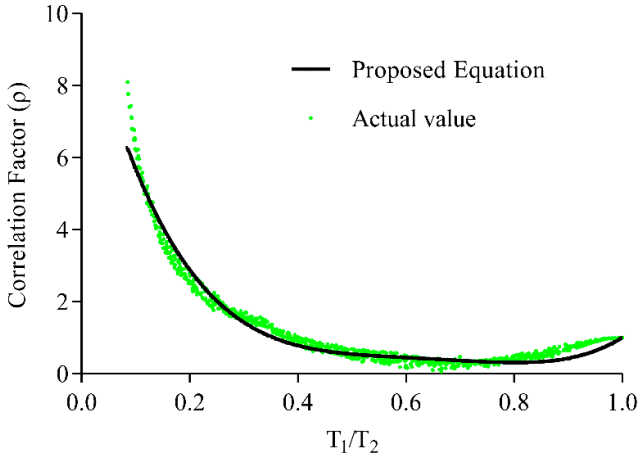

(**b**) $T_1 > 0.2$ s

Figure 5. Comparison between the actual trend and the proposed equation for the correlation factor when the colliding buildings are founded on soil type B.

2.3. Soil Type C

In this section, the proposed equation for the correlation factor when the colliding buildings are founded on soil type C is presented. Figure 6 presents the plot of the correlation factor when the colliding buildings are founded on soil type C versus T_1/T_2. It can be seen that the plot is a piecewise function, and it is composed of three different functions. It can also be noticed that the correlation factor follows three different trends depending on whether $T_1 \leq 0.2$ s, 0.2 s < $T_1 \leq 0.4$ s, or $T_1 > 0.4$ s (see Figure 6). Therefore, the proposed equation for the correlation factor when the colliding buildings are founded on soil type C is composed of three equations depending on whether $T_1 \leq 0.2$ s, 0.2 s < $T_1 \leq 0.4$ s, or $T_1 > 0.4$ s (see Equation (12)). Figure 7 shows a comparison between the proposed equation (Equation (12)) and the actual values of the correlation factor obtained for different cases. Using Equation (9), the RMS error has been calculated as equal to 7.00% for $T_1 \leq 0.2$ s, 2.98% for 0.2 s < $T_1 \leq 0.4$ s, and 6.31% for $T_1 > 0.4$ s.

$$\rho = \begin{cases} \left(\frac{T_1}{T_2}\right)^{-1.225} & , \ T_1 \leq 0.2 \text{ s} \\ 854.668\left(\frac{T_1}{T_2}\right)^6 - 3093\left(\frac{T_1}{T_2}\right)^5 + 4428.7\left(\frac{T_1}{T_2}\right)^4 - 3195.3\left(\frac{T_1}{T_2}\right)^3 + 1232.8\left(\frac{T_1}{T_2}\right)^2 & \\ \quad -250.62\left(\frac{T_1}{T_2}\right) + 23.752 & , \ 0.2\text{s} < T_1 \leq 0.4 \text{ s} \\ 18.95\left(\frac{T_1}{T_2}\right)^4 - 51.456\left(\frac{T_1}{T_2}\right)^3 + 58.036\left(\frac{T_1}{T_2}\right)^2 - 31.526\left(\frac{T_1}{T_2}\right) + 6.996 & , \ T_1 > 0.4 \text{ s} \end{cases} \quad (12)$$

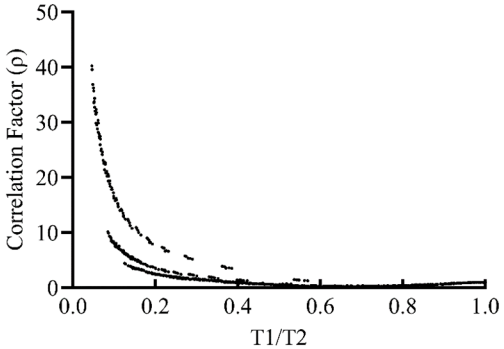

Figure 6. The correlation factor when the colliding buildings are founded on soil type C versus T_1/T_2. All lines correspond to the same thing (correlation factor). The graph of the correlation factor is not continuous.

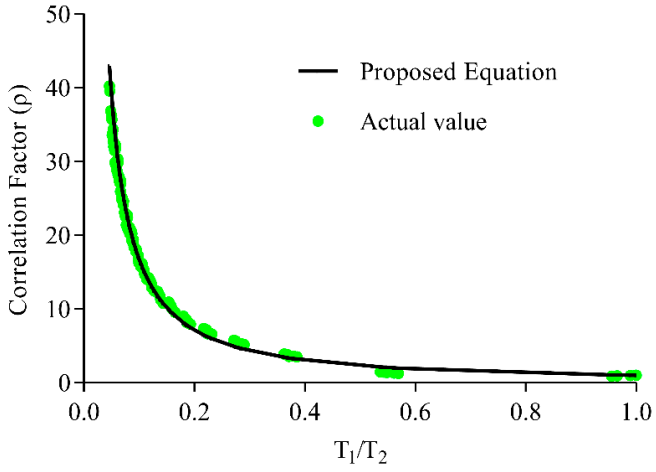

(**a**) $T_1 \leq 0.2$ s

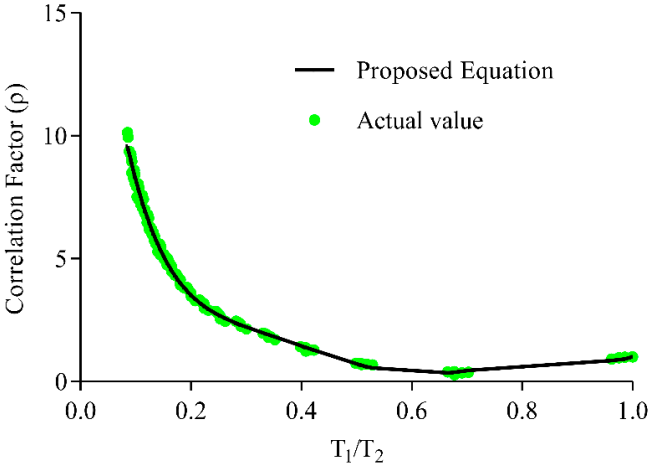

(**b**) 0.2 s < $T_1 \leq 0.4$ s

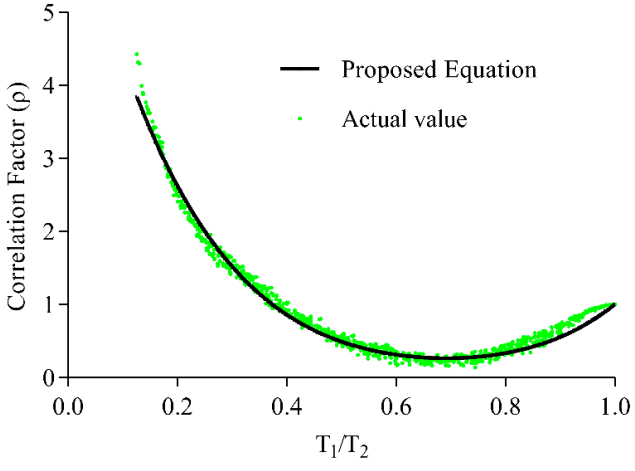

(**c**) $T_1 > 0.4$ s

Figure 7. Comparison between the actual trend and the proposed equation for the correlation factor when the colliding buildings are founded on soil type C.

2.4. Soil Type D

In this section, the proposed equation for the correlation factor when the colliding buildings are founded on soil type D is presented. Figure 8 presents the plot of the correlation factor when the colliding buildings are founded on soil type D versus T_1/T_2.

It can be seen that the plot is a piecewise function, and it is composed of three different functions. It can also be noticed that the correlation factor follows three different trends depending on whether $T_1 \leq 0.2$ s, 0.2 s < $T_1 \leq 0.4$ s, or $T_1 > 0.4$ s (see Figure 8). Therefore, the proposed equation for the correlation factor when the colliding buildings are founded on soil type D is composed of three equations depending on whether $T_1 \leq 0.2$ s, 0.2 s < $T_1 \leq 0.4$ s, or $T_1 > 0.4$ s (see Equation (13)). Figure 9 shows a comparison between the proposed equation (Equation (13)) and the actual values of the correlation factor obtained for different cases. Using Equation (9), the RMS error has been calculated as equal to 10.37% for $T_1 \leq 0.2$ s, 3.59% for 0.2 s < $T_1 \leq 0.4$ s, and 10.03% for $T_1 > 0.4$ s.

$$\rho = \begin{cases} \left(\frac{T_1}{T_2}\right)^{-1.295}, & T_1 \leq 0.2 \text{ s} \\ 732.762\left(\frac{T_1}{T_2}\right)^6 - 2675.9\left(\frac{T_1}{T_2}\right)^5 + 3882.2\left(\frac{T_1}{T_2}\right)^4 - 2859.2\left(\frac{T_1}{T_2}\right)^3 + 1142\left(\frac{T_1}{T_2}\right)^2 \\ \quad -246.34\left(\frac{T_1}{T_2}\right) + 25.478, \quad 0.2 \text{ s} < T_1 \leq 0.4 \text{ s} \\ 24.5342\left(\frac{T_1}{T_2}\right)^4 - 68.328\left(\frac{T_1}{T_2}\right)^3 + 76.198\left(\frac{T_1}{T_2}\right)^2 - 39.706\left(\frac{T_1}{T_2}\right) + 8.3018, \quad T_1 > 0.4 \text{ s} \end{cases} \tag{13}$$

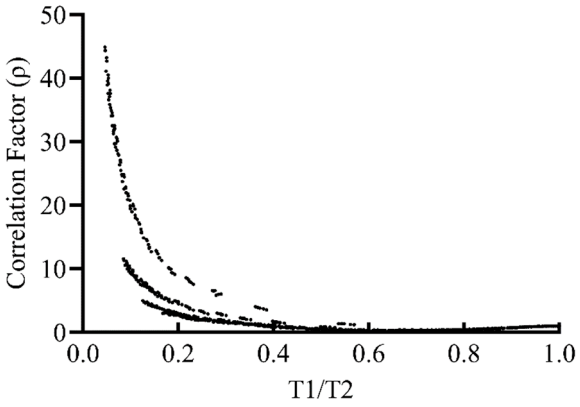

Figure 8. The correlation factor when the colliding buildings are founded on soil type D versus T_1/T_2. All lines correspond to the same thing (correlation factor). The graph of the correlation factor is not continuous.

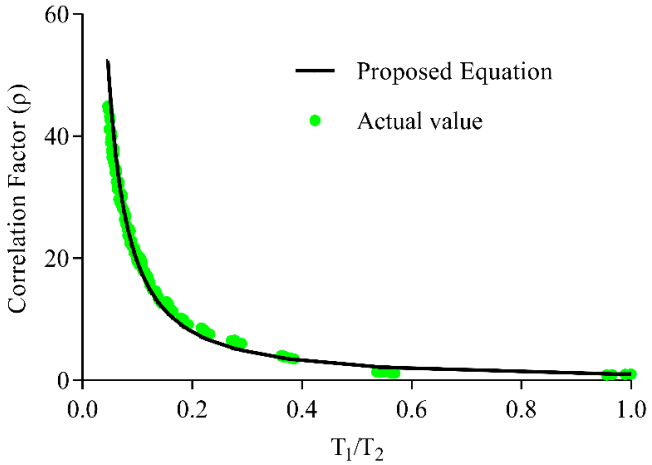

(**a**) $T_1 \leq 0.2$ s

Figure 9. *Cont.*

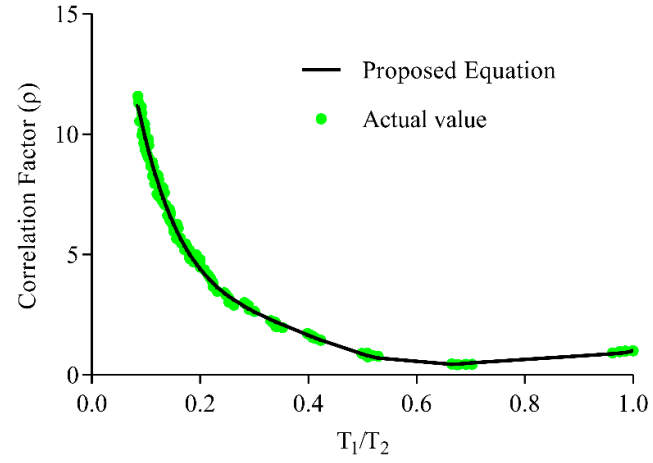

(**b**) 0.2 s < T_1 ≤ 0.4 s

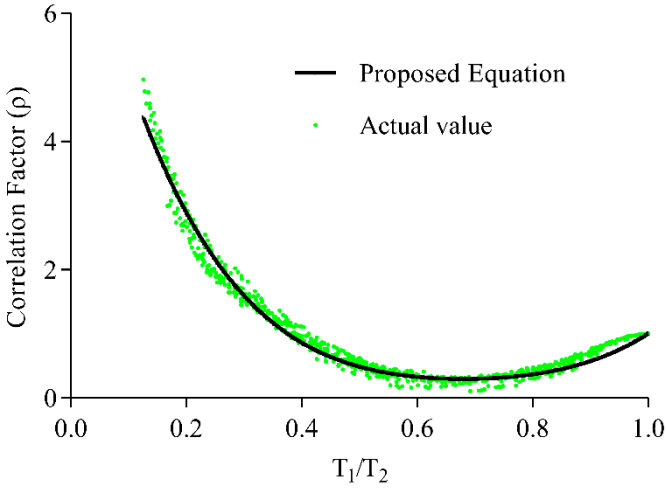

(**c**) T_1 > 0.4 s

Figure 9. Comparison between the actual trend and the proposed equation for the correlation factor when the colliding buildings are founded on soil type D.

2.5. Soil Type E

In this section, the proposed equation for the correlation factor when the colliding buildings are founded on soil type E is presented. Figure 10 presents the plot of the correlation factor when the colliding buildings are founded on soil type D versus T_1/T_2. It can be seen that the plot is a piecewise function, and it is composed of three different functions. It can also be noticed that the correlation factor follows three different trends depending on whether $T_1 \leq 0.2$ s, 0.2 s < $T_1 \leq 0.4$ s, or $T_1 > 0.4$ s (see Figure 10). Therefore, the proposed equation for the correlation factor when the colliding buildings are founded on soil type D is composed of three equations depending on whether $T_1 \leq 0.2$ s, 0.2 s < $T_1 \leq 0.4$ s, or $T_1 > 0.4$ s (see Equation (14)). Figure 11 shows a comparison between the proposed equation (Equation (14)) and the actual values of the correlation factor obtained for different cases. Using Equation (9), the RMS error has been calculated as equal to 7.00% for $T_1 \leq 0.2$ s, 2.98% for 0.2 s < $T_1 \leq 0.4$ s, and 8.30% for $T_1 > 0.4$ s. It should be noted at the end that, if the calculation based on the proposed correlation factors results in a negative value of the term $S^2 = {U_1}^2 + {U_2}^2 - 2\rho U_1 U_2$, then the absolute value should be taken into account for the calculation of the spacing S.

$$\rho = \begin{cases} \left(\frac{T_1}{T_2}\right)^{-1.519}, & T_1 \leq 0.2 \text{ s} \\ 2531.452\left(\frac{T_1}{T_2}\right)^6 - 8855.4\left(\frac{T_1}{T_2}\right)^5 + 12,190\left(\frac{T_1}{T_2}\right)^4 - 8404.1\left(\frac{T_1}{T_2}\right)^3 + 3076.1\left(\frac{T_1}{T_2}\right)^2 & \\ \quad -589.69\left(\frac{T_1}{T_2}\right) + 52.638, \quad 0.2 \text{ s} < T_1 \leq 0.4 \text{ s} & \\ 78.392\left(\frac{T_1}{T_2}\right)^4 - 214.39\left(\frac{T_1}{T_2}\right)^3 + 219.53\left(\frac{T_1}{T_2}\right)^2 - 99.972\left(\frac{T_1}{T_2}\right) + 17.44, & T_1 > 0.4 \text{ s} \end{cases} \quad (14)$$

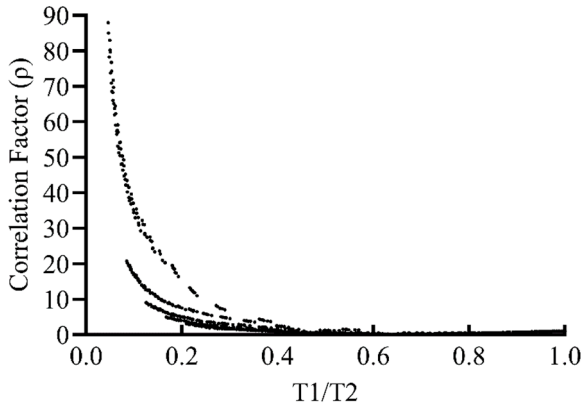

Figure 10. The correlation factor when the colliding buildings are founded on soil type E versus T_1/T_2. All lines correspond to the same thing (correlation factor). The graph of the correlation factor is not continuous.

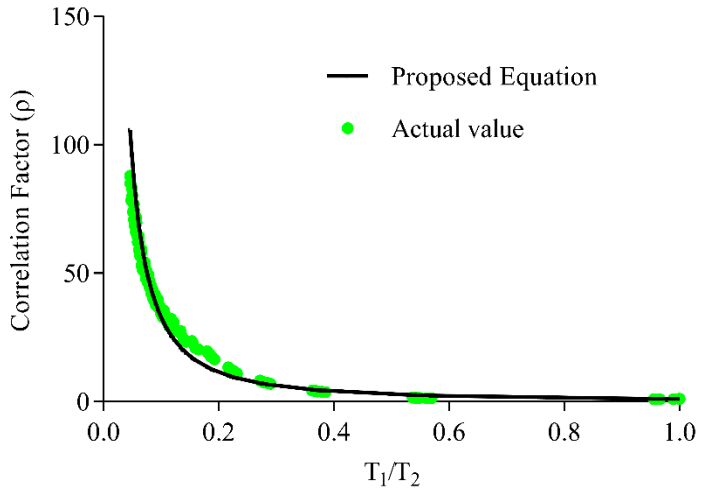

(**a**) $T_1 \leq 0.2$ s

Figure 11. *Cont.*

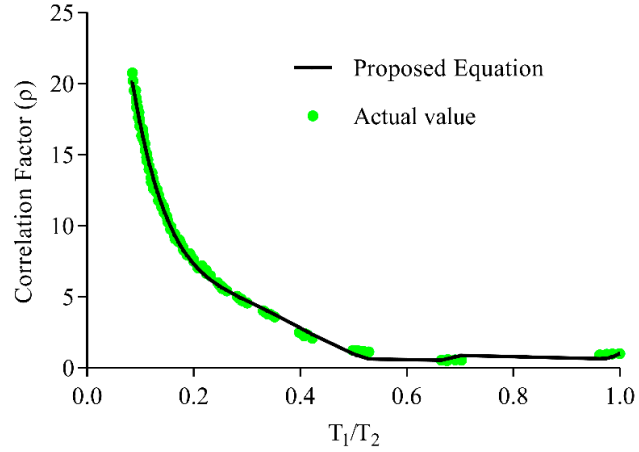

(**b**) 0.2 s < T_1 ≤ 0.4 s

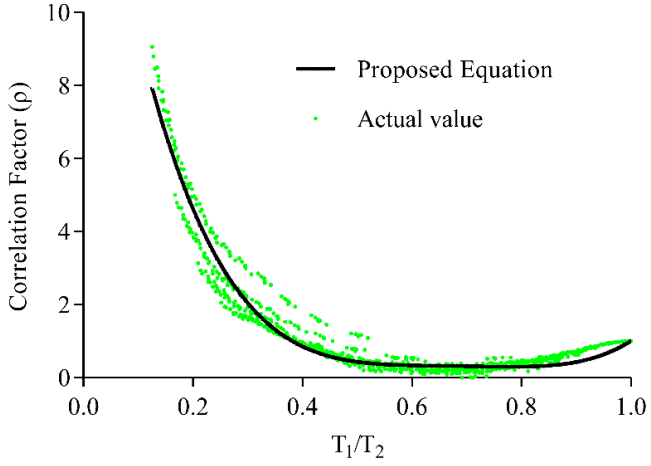

(**c**) T_1 > 0.4 s

Figure 11. Comparison between the actual trend and the proposed equation for the correlation factor when the colliding buildings are founded on soil type E.

3. Verification of the Effectiveness of the Proposed Equations

In this section, the effectiveness of the proposed equations is verified by comparing them with the equations existing in the literature. Table 4 considers a few pounding cases between buildings number 21–26 (see Table 1) founded on different soil types. Table 4 presents the exact required seismic gap to avoid collisions based on Equation (8), the gap calculated using equations proposed in this study, and the ratio between them. When this ratio is equal or close to 1, it means that the equation is accurate, while, when the ratio is much larger or much smaller than 1, it means that the equation is not accurate. It can be seen that the ratio of the gap using the equations proposed in this study and the exact required seismic gap to avoid collisions ranges between 0.99 and 1.34 and, in most cases, is close to 1. This means that the proposed equations are effective in calculating the accuracy of the seismic gap. Indeed, Table 5 presents the comparison between the seismic gap calculated using the ABS formula (Equation (1)) and the exact required seismic gap to avoid collisions based on Equation (8) as well as the ratio between them. It can be seen that the ratio of the gap calculated using the ABS formula and the exact required seismic gap to avoid collisions ranges between 1.55 and 3.74. This means that the ABS formula significantly overestimates the gap for the considered cases and the proposed equations provide better accuracy than the ABS formula. Also, Table 6 presents the comparison between the seismic gap calculated using the SRSS formula (Equation (2)) and the exact required seismic gap to avoid collisions based on Equation (8) as well as the ratio between them. It can be seen that the ratio of the

gap calculated using the SRSS formula and the exact required seismic gap to avoid collisions ranges between 1.18 and 3.53. This means that the SRSS formula significantly overestimates the gap for the considered cases and the proposed equations provide better accuracy than the SRSS formula. Also, Table 7 presents the comparison between the seismic gap calculated using the DDC formula (Equations (3) and (4)) and the exact required seismic gap to avoid collisions based on Equation (8) as well as the ratio between them. It can be seen that the ratio of the gap calculated using the DDC formula and the exact required seismic gap to avoid collisions ranges between 1.18 and 3.53. This means that the DDC formula significantly overestimates the gap for the considered cases and the proposed equations provide better accuracy than the DDC formula. Moreover, Table 8 presents the comparison between the seismic gap calculated using the Australian Code formula (Equation (5)) and the exact required seismic gap to avoid collisions based on Equation (8) as well as the ratio between them. It can be seen that the ratio of the gap calculated using the Australian Code formula and the exact required seismic gap to avoid collisions ranges between 0.74 and 14.81. This means that the Australian Code formula provides both accurate results as well as significantly overestimated results and the proposed equations provide better accuracy than the Australian Code formula. Furthermore, Table 9 presents the comparison between the seismic gap calculated using the Naderpour et al. [39] formula (Equations (4) and (6)) and the exact required seismic gap to avoid collisions based on Equation (8) as well as the ratio between them. It can be seen that the ratio of the gap calculated using the Naderpour et al. [39] formula and the exact required seismic gap to avoid collisions ranges between 1.43 and 3.88. This means that the Naderpour et al. [39] formula significantly overestimates the gap for the considered cases and the proposed equations provide better accuracy than the Naderpour et al. [39] formula. Miari and Jankowski [72] have extensively studied these formulas and it was found that these formulas provide accurate, underestimate, and overestimate results. The equations for the seismic gap proposed in this study aim to provide more accurate results.

Table 4. Comparison between the exact required gap and the gap evaluated by the proposed equations.

Building 1 Number	Building 2 Number	T_1 (s)	T_2 (s)	Soil Type	U_1 (mm)	U_2 (mm)	Exact Required Seismic Gap (mm)	Gap Based on the Proposed Equations (mm)	Ratio
21	22	0.2	0.36	A	2.56	11.41	4.05	4.63	1.14
21	23	0.2	0.53	B	7.82	54.16	19.58	20.33	1.04
21	23	0.2	0.53	C	8.28	71.12	28.59	33.6	1.18
21	23	0.2	0.53	D	8.34	71.51	28.9	28.94	1
21	24	0.2	0.7	E	6.98	113.98	32.37	43.38	1.34
22	23	0.36	0.53	A	11.41	43.8	32.57	40.73	1.25
22	23	0.36	0.53	B	31.31	54.16	49.56	50.91	1.03
22	23	0.36	0.53	C	31.97	71.12	60.4	66.01	1.09
22	25	0.36	0.88	D	30.84	145.17	79.7	88.05	1.1
22	24	0.36	0.7	E	28.3	113.98	89.55	90.23	1.01
24	25	0.7	0.88	A	56	73.14	77.84	76.95	0.99
24	25	0.7	0.88	B	69.78	90.94	94.14	95.75	1.02
24	25	0.7	0.88	C	96.83	117.13	103.02	124.54	1.21
24	25	0.7	0.88	D	111.74	145.17	144.09	146.96	1.02
24	26	0.7	1.06	E	113.98	261.62	241.92	249.35	1.03

Table 5. Comparison between the exact required gap and the gap evaluated by the ABS formula.

Building 1 Number	Building 2 Number	Soil Type	U_1 (mm)	U_2 (mm)	ABS (mm)	Required Gap (mm)	Ratio
21	22	A	2.56	11.41	13.97	4.05	3.45
21	23	B	7.82	54.16	61.97	19.58	3.17
21	23	C	8.28	71.12	79.39	28.59	2.78
21	23	D	8.34	71.51	79.85	28.90	2.76
21	24	E	6.98	113.98	120.96	32.37	3.74
22	23	A	11.41	43.80	55.21	32.57	1.69
22	23	B	31.31	54.16	85.47	49.56	1.72
22	23	C	31.97	71.12	103.08	60.40	1.71
22	25	D	30.84	145.17	176.01	79.70	2.21
22	24	E	28.30	113.98	142.28	89.55	1.59
24	25	A	56.00	73.14	129.14	77.84	1.66
24	25	B	69.78	90.94	160.72	94.14	1.71
24	25	C	96.83	117.13	213.95	103.02	2.08
24	25	D	111.74	145.17	256.91	144.09	1.78
24	26	E	113.98	261.62	375.61	241.92	1.55

Table 6. Comparison between the exact required gap and the gap evaluated by the SRSS formula.

Building 1 Number	Building 2 Number	Soil Type	U_1 (mm)	U_2 (mm)	SRSS (mm)	Required Gap (mm)	Ratio
21	22	A	2.56	11.41	11.69	4.05	2.89
21	23	B	7.82	54.16	54.72	19.58	2.80
21	23	C	8.28	71.12	71.59	28.59	2.50
21	23	D	8.34	71.51	71.99	28.90	2.49
21	24	E	6.98	113.98	114.19	32.37	3.53
22	23	A	11.41	43.80	45.26	32.57	1.39
22	23	B	31.31	54.16	62.56	49.56	1.26
22	23	C	31.97	71.12	77.97	60.40	1.29
22	25	D	30.84	145.17	148.41	79.70	1.86
22	24	E	28.30	113.98	117.44	89.55	1.31
24	25	A	56.00	73.14	92.12	77.84	1.18
24	25	B	69.78	90.94	114.63	94.14	1.22
24	25	C	96.83	117.13	151.97	103.02	1.48
24	25	D	111.74	145.17	183.19	144.09	1.27
24	26	E	113.98	261.62	285.37	241.92	1.18

Table 7. Comparison between the exact required gap and the gap evaluated by the DDC formula.

Building 1 Number	Building 2 Number	Soil Type	U_1 (mm)	U_2 (mm)	DDC (mm)	Required Gap (mm)	Ratio
21	22	A	2.56	11.41	11.63	4.05	2.87
21	23	B	7.82	54.16	54.66	19.58	2.79
21	23	C	8.28	71.12	71.53	28.59	2.50
21	23	D	8.34	71.51	71.92	28.90	2.49
21	24	E	6.98	113.98	114.16	32.37	3.53
22	23	A	11.41	43.80	44.60	32.57	1.37
22	23	B	31.31	54.16	60.92	49.56	1.23
22	23	C	31.97	71.12	76.21	60.40	1.26
22	25	D	30.84	145.17	148.10	79.70	1.86
22	24	E	28.30	113.98	116.90	89.55	1.31
24	25	A	56.00	73.14	84.45	77.84	1.08
24	25	B	69.78	90.94	105.08	94.14	1.12
24	25	C	96.83	117.13	139.09	103.02	1.35
24	25	D	111.74	145.17	167.92	144.09	1.17
24	26	E	113.98	261.62	279.56	241.92	1.16

Table 8. Comparison between the exact required gap and the gap evaluated by the Australian Code formula.

Building 1 Number	Building 2 Number	Soil Type	U_1 (mm)	U_2 (mm)	Australian Code Formula (mm)	Required Gap (mm)	Ratio
21	22	A	2.6	11.4	60.0	4.1	14.81
21	23	B	7.8	54.2	90.0	19.6	4.60
21	23	C	8.3	71.1	90.0	28.6	3.15
21	23	D	8.34	71.51	90.0	28.90	3.11
21	24	E	6.98	113.98	120.0	32.37	3.71
22	23	A	11.41	43.80	90.0	32.57	2.76
22	23	B	31.31	54.16	90.0	49.56	1.82
22	23	C	31.97	71.12	90.0	60.40	1.49
22	25	D	30.84	145.17	150.0	79.70	1.88
22	24	E	28.30	113.98	120.0	89.55	1.34
24	25	A	56.00	73.14	150.0	77.84	1.93
24	25	B	69.78	90.94	150.0	94.14	1.59
24	25	C	96.83	117.13	150.0	103.02	1.46
24	25	D	111.74	145.17	150.0	144.09	1.04
24	26	E	113.98	261.62	180.0	241.92	0.74

Table 9. Comparison between the exact required gap and the gap evaluated by the Naderpour et al. [39] formula.

Building 1 Number	Building 2 Number	Soil Type	U_1 (mm)	U_2 (mm)	Naderpour et al. (mm)	Required Gap (mm)	Ratio
21	22	A	2.6	11.4	11.4	4.1	2.81
21	23	B	7.8	54.2	60.6	19.6	3.09
21	23	C	8.3	71.1	77.8	28.6	2.72
21	23	D	8.34	71.51	78.30	28.90	2.71
21	24	E	6.98	113.98	125.66	32.37	3.88
22	23	A	11.41	43.80	48.64	32.57	1.49
22	23	B	31.31	54.16	70.65	49.56	1.43
22	23	C	31.97	71.12	86.74	60.40	1.44
22	25	D	30.84	145.17	221.42	79.70	2.78
22	24	E	28.30	113.98	156.51	89.55	1.75
24	25	A	56.00	73.14	115.68	77.84	1.49
24	25	B	69.78	90.94	143.96	94.14	1.53
24	25	C	96.83	117.13	191.44	103.02	1.86
24	25	D	111.74	145.17	230.11	144.09	1.60
24	26	E	113.98	261.62	461.42	241.92	1.91

4. Conclusions

In this paper, new equations for the evaluation of the optimum seismic gap preventing earthquake-induced pounding between adjacent buildings founded on different soil conditions have been proposed. The DDC formula has been taken into consideration and the modification of the correlation factor has been introduced. In the study, 1260 cases of pounding between different concrete buildings with various dynamic properties have been considered under five ground motions. Five soil types have been taken into account, as defined in the ASCE 7-10 code [69], i.e., hard rock, rock, very dense soil and soft rock, stiff soil, and soft clay soil. The normalized RMS errors have been calculated for the proposed equations. The results of the study indicate that the error ranges between 2% and 14%, confirming the accuracy of the approach. Therefore, the proposed equations can be effectively used for the determination of the optimum seismic gap preventing earthquake-induced pounding between buildings founded on different soil types. The current equations existing in the literature consider only one equation for the separation distance regardless of the soil type, which means that the same equation is supposed to be valid no matter the soil type. However, the proposed equations are multiple equations where every equation corresponds to a certain soil type, which means that the selection of the equation to be used is dependent on the soil type that the buildings are founded on. By designing the buildings and providing separation between them based on the proposed equations, no collisions will occur between them, which means that providing spacing based on the proposed equations will provide more safety to the vibrating buildings during earthquakes. Since only concrete buildings are considered in this study, it can be said that the accuracy of the formulas is verified for concrete buildings and for concrete-to-concrete pounding. The accuracy of these formulas has to be investigated for other kinds of pounding, such as steel-to-steel pounding and timber-to-timber pounding, and compared with the formulas existing in the literature. The current formulas existing in the literature can be less or more accurate than the proposed equations in other kinds of pounding, such as steel-to-steel pounding and timber-to-timber pounding. Since the equations are based on natural periods, they should also be valid for steel and timber structures. However, further checking and verification

are necessary. Also, checking the accuracy of the proposed equations compared with the current formulas existing in the literature in the case of direct integration nonlinear analyses rather than fast nonlinear analyses (FNAs) is required. Finally, an experimental verification of the proposed equations is necessary. The experimental verification can be completed using the shaking table by simulating two models placed with a separation distance based on the proposed equations and checking if pounding occurs or not.

Author Contributions: M.M.: Conceptualization, Methodology, Formal analysis, Investigation, Writing—Original Draft. R.J.: Supervision, Writing—Review & Editing. All authors have read and agreed to the published version of the manuscript.

Funding: The first author (Mahmoud Miari) gratefully acknowledges the financial support of this research from the "Doctoral Scholarship" awarded from Gdańsk University of Technology.

Institutional Review Board Statement: Not applicable.

Informed Consent Statement: Not applicable.

Data Availability Statement: All the data are included in the article.

Conflicts of Interest: The authors declare no conflict of interest.

Appendix A

Table A1. Pounding cases considered in this study.

Pounding Case	Building 1	Building 2	Period Ratio
1	1	1	1.000
2	1	2	0.548
3	1	3	0.372
4	1	4	0.280
5	1	5	0.224
6	1	6	0.186
7	1	7	0.159
8	1	8	0.139
9	1	9	0.123
10	1	10	0.110
11	1	11	0.100
12	1	12	0.091
13	1	13	0.083
14	1	14	0.077
15	1	15	0.071
16	1	16	0.066
17	1	17	0.062
18	1	18	0.058
19	1	19	0.054
20	1	20	0.051
21	1	21	1.046
22	1	22	0.570
23	1	23	0.386
24	1	24	0.290
25	1	25	0.232

Table A1. *Cont.*

Pounding Case	Building 1	Building 2	Period Ratio
26	1	26	0.193
27	1	27	0.165
28	1	28	0.144
29	1	29	0.127
30	1	30	0.114
31	1	31	0.103
32	1	32	0.094
33	1	33	0.086
34	1	34	0.079
35	1	35	0.074
36	1	36	0.068
37	1	37	0.064
38	1	38	0.060
39	1	39	0.056
40	1	40	0.053
41	1	41	1.036
42	1	42	0.562
43	1	43	0.379
44	1	44	0.285
45	1	45	0.227
46	1	46	0.189
47	1	47	0.161
48	1	48	0.140
49	1	49	0.123
50	1	50	0.110
51	1	51	0.099
52	1	52	0.090
53	1	53	0.082
54	1	54	0.075
55	1	55	0.069
56	1	56	0.064
57	1	57	0.060
58	1	58	0.056
59	1	59	0.052
60	1	60	0.049
61	2	2	1.000
62	2	3	0.678
63	2	4	0.510
64	2	5	0.409
65	2	6	0.340
66	2	7	0.291

Table A1. *Cont.*

Pounding Case	Building 1	Building 2	Period Ratio
67	2	8	0.254
68	2	9	0.224
69	2	10	0.201
70	2	11	0.182
71	2	12	0.166
72	2	13	0.152
73	2	14	0.140
74	2	15	0.130
75	2	16	0.121
76	2	17	0.113
77	2	18	0.105
78	2	19	0.099
79	2	20	0.093
80	2	22	1.039
81	2	23	0.703
82	2	24	0.529
83	2	25	0.423
84	2	26	0.352
85	2	27	0.301
86	2	28	0.262
87	2	29	0.232
88	2	30	0.208
89	2	31	0.188
90	2	32	0.171
91	2	33	0.157
92	2	34	0.145
93	2	35	0.134
94	2	36	0.125
95	2	37	0.117
96	2	38	0.109
97	2	39	0.103
98	2	40	0.097
99	2	42	1.025
100	2	43	0.691
101	2	44	0.519
102	2	45	0.414
103	2	46	0.344
104	2	47	0.293
105	2	48	0.255
106	2	49	0.225
107	2	50	0.200

Table A1. *Cont.*

Pounding Case	Building 1	Building 2	Period Ratio
108	2	51	0.180
109	2	52	0.164
110	2	53	0.149
111	2	54	0.137
112	2	55	0.127
113	2	56	0.117
114	2	57	0.109
115	2	58	0.101
116	2	59	0.095
117	2	60	0.089
118	3	3	1.000
119	3	4	0.753
120	3	5	0.603
121	3	6	0.502
122	3	7	0.429
123	3	8	0.374
124	3	9	0.331
125	3	10	0.297
126	3	11	0.268
127	3	12	0.244
128	3	13	0.224
129	3	14	0.207
130	3	15	0.191
131	3	16	0.178
132	3	17	0.166
133	3	18	0.156
134	3	19	0.146
135	3	20	0.138
136	3	23	1.038
137	3	24	0.781
138	3	25	0.625
139	3	26	0.520
140	3	27	0.444
141	3	28	0.387
142	3	29	0.343
143	3	30	0.307
144	3	31	0.277
145	3	32	0.253
146	3	33	0.232
147	3	34	0.214
148	3	35	0.198

Table A1. *Cont.*

Pounding Case	Building 1	Building 2	Period Ratio
149	3	36	0.184
150	3	37	0.172
151	3	38	0.161
152	3	39	0.151
153	3	40	0.142
154	3	43	1.020
155	3	44	0.766
156	3	45	0.611
157	3	46	0.507
158	3	47	0.432
159	3	48	0.376
160	3	49	0.331
161	3	50	0.296
162	3	51	0.266
163	3	52	0.242
164	3	53	0.221
165	3	54	0.203
166	3	55	0.187
167	3	56	0.173
168	3	57	0.161
169	3	58	0.150
170	3	59	0.140
171	3	60	0.131
172	4	4	1.000
173	4	5	0.801
174	4	6	0.666
175	4	7	0.570
176	4	8	0.497
177	4	9	0.440
178	4	10	0.394
179	4	11	0.356
180	4	12	0.324
181	4	13	0.298
182	4	14	0.274
183	4	15	0.254
184	4	16	0.236
185	4	17	0.221
186	4	18	0.207
187	4	19	0.194
188	4	20	0.183
189	4	24	1.037

Table A1. *Cont.*

Pounding Case	Building 1	Building 2	Period Ratio
190	4	25	0.829
191	4	26	0.690
192	4	27	0.590
193	4	28	0.514
194	4	29	0.455
195	4	30	0.407
196	4	31	0.368
197	4	32	0.336
198	4	33	0.308
199	4	34	0.284
200	4	35	0.263
201	4	36	0.245
202	4	37	0.228
203	4	38	0.214
204	4	39	0.201
205	4	40	0.189
206	4	44	1.017
207	4	45	0.812
208	4	46	0.674
209	4	47	0.574
210	4	48	0.499
211	4	49	0.440
212	4	50	0.393
213	4	51	0.354
214	4	52	0.321
215	4	53	0.293
216	4	54	0.269
217	4	55	0.248
218	4	56	0.230
219	4	57	0.213
220	4	58	0.199
221	4	59	0.186
222	4	60	0.174
223	5	5	1.000
224	5	6	0.832
225	5	7	0.711
226	5	8	0.620
227	5	9	0.549
228	5	10	0.492
229	5	11	0.444
230	5	12	0.405

Table A1. *Cont.*

Pounding Case	Building 1	Building 2	Period Ratio
231	5	13	0.371
232	5	14	0.342
233	5	15	0.317
234	5	16	0.295
235	5	17	0.276
236	5	18	0.258
237	5	19	0.242
238	5	20	0.228
239	5	25	1.035
240	5	26	0.862
241	5	27	0.736
242	5	28	0.642
243	5	29	0.568
244	5	30	0.509
245	5	31	0.460
246	5	32	0.419
247	5	33	0.384
248	5	34	0.354
249	5	35	0.328
250	5	36	0.305
251	5	37	0.285
252	5	38	0.267
253	5	39	0.251
254	5	40	0.236
255	5	45	1.013
256	5	46	0.841
257	5	47	0.717
258	5	48	0.623
259	5	49	0.549
260	5	50	0.490
261	5	51	0.441
262	5	52	0.401
263	5	53	0.366
264	5	54	0.336
265	5	55	0.310
266	5	56	0.287
267	5	57	0.266
268	5	58	0.248
269	5	59	0.232
270	5	60	0.217
271	6	6	1.000

Table A1. *Cont.*

Pounding Case	Building 1	Building 2	Period Ratio
272	6	7	0.855
273	6	8	0.746
274	6	9	0.660
275	6	10	0.591
276	6	11	0.534
277	6	12	0.487
278	6	13	0.447
279	6	14	0.412
280	6	15	0.381
281	6	16	0.355
282	6	17	0.331
283	6	18	0.310
284	6	19	0.291
285	6	20	0.274
286	6	26	1.036
287	6	27	0.885
288	6	28	0.772
289	6	29	0.683
290	6	30	0.612
291	6	31	0.553
292	6	32	0.504
293	6	33	0.462
294	6	34	0.426
295	6	35	0.395
296	6	36	0.367
297	6	37	0.343
298	6	38	0.321
299	6	39	0.302
300	6	40	0.284
301	6	46	1.011
302	6	47	0.861
303	6	48	0.749
304	6	49	0.660
305	6	50	0.589
306	6	51	0.531
307	6	52	0.482
308	6	53	0.440
309	6	54	0.404
310	6	55	0.372
311	6	56	0.344
312	6	57	0.320

Table A1. *Cont.*

Pounding Case	Building 1	Building 2	Period Ratio
313	6	58	0.298
314	6	59	0.278
315	6	60	0.261
316	7	7	1.000
317	7	8	0.872
318	7	9	0.771
319	7	10	0.691
320	7	11	0.625
321	7	12	0.569
322	7	13	0.522
323	7	14	0.481
324	7	15	0.446
325	7	16	0.415
326	7	17	0.387
327	7	18	0.363
328	7	19	0.340
329	7	20	0.320
330	7	27	1.035
331	7	28	0.902
332	7	29	0.798
333	7	30	0.715
334	7	31	0.646
335	7	32	0.589
336	7	33	0.540
337	7	34	0.498
338	7	35	0.462
339	7	36	0.429
340	7	37	0.401
341	7	38	0.375
342	7	39	0.353
343	7	40	0.332
344	7	47	1.007
345	7	48	0.875
346	7	49	0.772
347	7	50	0.689
348	7	51	0.620
349	7	52	0.563
350	7	53	0.514
351	7	54	0.472
352	7	55	0.435
353	7	56	0.403

Table A1. *Cont.*

Pounding Case	Building 1	Building 2	Period Ratio
354	7	57	0.374
355	7	58	0.348
356	7	59	0.326
357	7	60	0.305
358	8	8	1.000
359	8	9	0.885
360	8	10	0.793
361	8	11	0.716
362	8	12	0.653
363	8	13	0.599
364	8	14	0.552
365	8	15	0.512
366	8	16	0.476
367	8	17	0.444
368	8	18	0.416
369	8	19	0.390
370	8	20	0.368
371	8	28	1.035
372	8	29	0.916
373	8	30	0.820
374	8	31	0.741
375	8	32	0.676
376	8	33	0.620
377	8	34	0.571
378	8	35	0.529
379	8	36	0.492
380	8	37	0.460
381	8	38	0.431
382	8	39	0.404
383	8	40	0.381
384	8	48	1.004
385	8	49	0.885
386	8	50	0.790
387	8	51	0.711
388	8	52	0.646
389	8	53	0.589
390	8	54	0.541
391	8	55	0.499
392	8	56	0.462
393	8	57	0.429
394	8	58	0.400

Table A1. *Cont.*

Pounding Case	Building 1	Building 2	Period Ratio
395	8	59	0.373
396	8	60	0.350
397	9	9	1.000
398	9	10	0.896
399	9	11	0.810
400	9	12	0.738
401	9	13	0.677
402	9	14	0.624
403	9	15	0.578
404	9	16	0.538
405	9	17	0.502
406	9	18	0.470
407	9	19	0.441
408	9	20	0.415
409	9	29	1.035
410	9	30	0.927
411	9	31	0.838
412	9	32	0.764
413	9	33	0.700
414	9	34	0.646
415	9	35	0.598
416	9	36	0.557
417	9	37	0.520
418	9	38	0.487
419	9	39	0.457
420	9	40	0.430
421	9	49	1.001
422	9	50	0.893
423	9	51	0.804
424	9	52	0.730
425	9	53	0.666
426	9	54	0.612
427	9	55	0.564
428	9	56	0.522
429	9	57	0.485
430	9	58	0.452
431	9	59	0.422
432	9	60	0.395
433	10	10	1.000
434	10	11	0.904
435	10	12	0.824

Table A1. *Cont.*

Pounding Case	Building 1	Building 2	Period Ratio
436	10	13	0.756
437	10	14	0.697
438	10	15	0.645
439	10	16	0.600
440	10	17	0.560
441	10	18	0.525
442	10	19	0.493
443	10	20	0.464
444	10	30	1.035
445	10	31	0.935
446	10	32	0.853
447	10	33	0.782
448	10	34	0.721
449	10	35	0.668
450	10	36	0.621
451	10	37	0.580
452	10	38	0.543
453	10	39	0.510
454	10	40	0.480
455	10	50	0.997
456	10	51	0.898
457	10	52	0.815
458	10	53	0.744
459	10	54	0.683
460	10	55	0.630
461	10	56	0.583
462	10	57	0.541
463	10	58	0.504
464	10	59	0.471
465	10	60	0.441
466	11	11	1.000
467	11	12	0.911
468	11	13	0.836
469	11	14	0.771
470	11	15	0.714
471	11	16	0.664
472	11	17	0.620
473	11	18	0.580
474	11	19	0.545
475	11	20	0.513
476	11	31	1.035

Table A1. *Cont.*

Pounding Case	Building 1	Building 2	Period Ratio
477	11	32	0.943
478	11	33	0.865
479	11	34	0.798
480	11	35	0.739
481	11	36	0.687
482	11	37	0.642
483	11	38	0.601
484	11	39	0.564
485	11	40	0.532
486	11	51	0.993
487	11	52	0.901
488	11	53	0.823
489	11	54	0.755
490	11	55	0.697
491	11	56	0.645
492	11	57	0.599
493	11	58	0.558
494	11	59	0.521
495	11	60	0.488
496	12	12	1.000
497	12	13	0.917
498	12	14	0.846
499	12	15	0.783
500	12	16	0.729
501	12	17	0.680
502	12	18	0.637
503	12	19	0.598
504	12	20	0.563
505	12	32	1.035
506	12	33	0.949
507	12	34	0.875
508	12	35	0.811
509	12	36	0.754
510	12	37	0.704
511	12	38	0.660
512	12	39	0.619
513	12	40	0.583
514	12	52	0.989
515	12	53	0.903
516	12	54	0.829
517	12	55	0.764

Table A1. *Cont.*

Pounding Case	Building 1	Building 2	Period Ratio
518	12	56	0.707
519	12	57	0.657
520	12	58	0.612
521	12	59	0.572
522	12	60	0.536
523	13	13	1.000
524	13	14	0.922
525	13	15	0.854
526	13	16	0.794
527	13	17	0.742
528	13	18	0.694
529	13	19	0.652
530	13	20	0.614
531	13	33	1.035
532	13	34	0.954
533	13	35	0.884
534	13	36	0.822
535	13	37	0.768
536	13	38	0.719
537	13	39	0.675
538	13	40	0.636
539	13	53	0.984
540	13	54	0.904
541	13	55	0.833
542	13	56	0.771
543	13	57	0.716
544	13	58	0.667
545	13	59	0.624
546	13	60	0.584
547	14	14	1.000
548	14	15	0.926
549	14	16	0.862
550	14	17	0.804
551	14	18	0.753
552	14	19	0.707
553	14	20	0.666
554	14	34	1.035
555	14	35	0.959
556	14	36	0.892
557	14	37	0.833
558	14	38	0.780

Table A1. *Cont.*

Pounding Case	Building 1	Building 2	Period Ratio
559	14	39	0.732
560	14	40	0.690
561	14	54	0.980
562	14	55	0.904
563	14	56	0.837
564	14	57	0.777
565	14	58	0.724
566	14	59	0.676
567	14	60	0.633
568	15	15	1.000
569	15	16	0.930
570	15	17	0.868
571	15	18	0.813
572	15	19	0.763
573	15	20	0.719
574	15	35	1.035
575	15	36	0.963
576	15	37	0.899
577	15	38	0.842
578	15	39	0.791
579	15	40	0.744
580	15	55	0.976
581	15	56	0.903
582	15	57	0.839
583	15	58	0.781
584	15	59	0.730
585	15	60	0.684
586	16	16	1.000
587	16	17	0.934
588	16	18	0.874
589	16	19	0.821
590	16	20	0.773
591	16	36	1.035
592	16	37	0.966
593	16	38	0.905
594	16	39	0.850
595	16	40	0.800
596	16	56	0.971
597	16	57	0.902
598	16	58	0.840
599	16	59	0.785

Table A1. *Cont.*

Pounding Case	Building 1	Building 2	Period Ratio
600	16	60	0.735
601	17	17	1.000
602	17	18	0.936
603	17	19	0.879
604	17	20	0.828
605	17	37	1.035
606	17	38	0.969
607	17	39	0.910
608	17	40	0.857
609	17	57	0.966
610	17	58	0.900
611	17	59	0.841
612	17	60	0.787
613	18	18	1.000
614	18	19	0.939
615	18	20	0.884
616	18	38	1.036
617	18	39	0.972
618	18	40	0.916
619	18	58	0.961
620	18	59	0.898
621	18	60	0.841
622	19	19	1.000
623	19	20	0.941
624	19	39	1.036
625	19	40	0.975
626	19	59	0.956
627	19	60	0.895
628	20	20	1.000
629	20	40	1.036
630	20	60	0.951
631	21	21	1.000
632	21	22	0.545
633	21	23	0.369
634	21	24	0.277
635	21	25	0.222
636	21	26	0.185
637	21	27	0.158
638	21	28	0.138
639	21	29	0.122
640	21	30	0.109

Table A1. *Cont.*

Pounding Case	Building 1	Building 2	Period Ratio
641	21	31	0.099
642	21	32	0.090
643	21	33	0.082
644	21	34	0.076
645	21	35	0.070
646	21	36	0.065
647	21	37	0.061
648	21	38	0.057
649	21	39	0.054
650	21	40	0.051
651	21	41	0.990
652	21	42	0.537
653	21	43	0.362
654	21	44	0.272
655	21	45	0.217
656	21	46	0.180
657	21	47	0.154
658	21	48	0.133
659	21	49	0.118
660	21	50	0.105
661	21	51	0.095
662	21	52	0.086
663	21	53	0.078
664	21	54	0.072
665	21	55	0.066
666	21	56	0.061
667	21	57	0.057
668	21	58	0.053
669	21	59	0.050
670	21	60	0.046
671	22	22	1.000
672	22	23	0.677
673	22	24	0.509
674	22	25	0.407
675	22	26	0.339
676	22	27	0.290
677	22	28	0.252
678	22	29	0.223
679	22	30	0.200
680	22	31	0.181
681	22	32	0.165

Table A1. *Cont.*

Pounding Case	Building 1	Building 2	Period Ratio
682	22	33	0.151
683	22	34	0.139
684	22	35	0.129
685	22	36	0.120
686	22	37	0.112
687	22	38	0.105
688	22	39	0.099
689	22	40	0.093
690	22	42	0.986
691	22	43	0.665
692	22	44	0.499
693	22	45	0.399
694	22	46	0.331
695	22	47	0.282
696	22	48	0.245
697	22	49	0.216
698	22	50	0.193
699	22	51	0.174
700	22	52	0.158
701	22	53	0.144
702	22	54	0.132
703	22	55	0.122
704	22	56	0.113
705	22	57	0.105
706	22	58	0.098
707	22	59	0.091
708	22	60	0.085
709	23	23	1.000
710	23	24	0.752
711	23	25	0.602
712	23	26	0.501
713	23	27	0.428
714	23	28	0.373
715	23	29	0.330
716	23	30	0.296
717	23	31	0.267
718	23	32	0.244
719	23	33	0.223
720	23	34	0.206
721	23	35	0.191
722	23	36	0.178

Table A1. *Cont.*

Pounding Case	Building 1	Building 2	Period Ratio
723	23	37	0.166
724	23	38	0.155
725	23	39	0.146
726	23	40	0.137
727	23	43	0.983
728	23	44	0.738
729	23	45	0.589
730	23	46	0.489
731	23	47	0.417
732	23	48	0.362
733	23	49	0.319
734	23	50	0.285
735	23	51	0.257
736	23	52	0.233
737	23	53	0.213
738	23	54	0.195
739	23	55	0.180
740	23	56	0.167
741	23	57	0.155
742	23	58	0.144
743	23	59	0.135
744	23	60	0.126
745	24	24	1.000
746	24	25	0.800
747	24	26	0.666
748	24	27	0.569
749	24	28	0.496
750	24	29	0.439
751	24	30	0.393
752	24	31	0.355
753	24	32	0.324
754	24	33	0.297
755	24	34	0.274
756	24	35	0.254
757	24	36	0.236
758	24	37	0.220
759	24	38	0.206
760	24	39	0.194
761	24	40	0.182
762	24	44	0.980
763	24	45	0.783

Table A1. *Cont.*

Pounding Case	Building 1	Building 2	Period Ratio
764	24	46	0.650
765	24	47	0.554
766	24	48	0.481
767	24	49	0.424
768	24	50	0.379
769	24	51	0.341
770	24	52	0.309
771	24	53	0.282
772	24	54	0.259
773	24	55	0.239
774	24	56	0.221
775	24	57	0.206
776	24	58	0.192
777	24	59	0.179
778	24	60	0.168
779	25	25	1.000
780	25	26	0.832
781	25	27	0.711
782	25	28	0.620
783	25	29	0.549
784	25	30	0.491
785	25	31	0.444
786	25	32	0.405
787	25	33	0.371
788	25	34	0.342
789	25	35	0.317
790	25	36	0.295
791	25	37	0.275
792	25	38	0.258
793	25	39	0.242
794	25	40	0.228
795	25	45	0.979
796	25	46	0.812
797	25	47	0.692
798	25	48	0.602
799	25	49	0.530
800	25	50	0.473
801	25	51	0.426
802	25	52	0.387
803	25	53	0.353
804	25	54	0.324

Table A1. *Cont.*

Pounding Case	Building 1	Building 2	Period Ratio
805	25	55	0.299
806	25	56	0.277
807	25	57	0.257
808	25	58	0.239
809	25	59	0.224
810	25	60	0.209
811	26	26	1.000
812	26	27	0.854
813	26	28	0.745
814	26	29	0.659
815	26	30	0.590
816	26	31	0.534
817	26	32	0.486
818	26	33	0.446
819	26	34	0.411
820	26	35	0.381
821	26	36	0.354
822	26	37	0.331
823	26	38	0.310
824	26	39	0.291
825	26	40	0.274
826	26	46	0.976
827	26	47	0.831
828	26	48	0.723
829	26	49	0.637
830	26	50	0.569
831	26	51	0.512
832	26	52	0.465
833	26	53	0.424
834	26	54	0.390
835	26	55	0.359
836	26	56	0.332
837	26	57	0.309
838	26	58	0.288
839	26	59	0.269
840	26	60	0.252
841	27	27	1.000
842	27	28	0.872
843	27	29	0.772
844	27	30	0.691
845	27	31	0.625

Table A1. *Cont.*

Pounding Case	Building 1	Building 2	Period Ratio
846	27	32	0.569
847	27	33	0.522
848	27	34	0.481
849	27	35	0.446
850	27	36	0.415
851	27	37	0.387
852	27	38	0.363
853	27	39	0.341
854	27	40	0.321
855	27	47	0.973
856	27	48	0.846
857	27	49	0.746
858	27	50	0.666
859	27	51	0.599
860	27	52	0.544
861	27	53	0.497
862	27	54	0.456
863	27	55	0.420
864	27	56	0.389
865	27	57	0.361
866	27	58	0.337
867	27	59	0.315
868	27	60	0.295
869	28	28	1.000
870	28	29	0.885
871	28	30	0.793
872	28	31	0.717
873	28	32	0.653
874	28	33	0.599
875	28	34	0.552
876	28	35	0.512
877	28	36	0.476
878	28	37	0.444
879	28	38	0.416
880	28	39	0.391
881	28	40	0.368
882	28	48	0.971
883	28	49	0.856
884	28	50	0.764
885	28	51	0.688
886	28	52	0.624

Table A1. *Cont.*

Pounding Case	Building 1	Building 2	Period Ratio
887	28	53	0.570
888	28	54	0.523
889	28	55	0.482
890	28	56	0.446
891	28	57	0.415
892	28	58	0.386
893	28	59	0.361
894	28	60	0.338
895	29	29	1.000
896	29	30	0.895
897	29	31	0.809
898	29	32	0.738
899	29	33	0.677
900	29	34	0.624
901	29	35	0.578
902	29	36	0.538
903	29	37	0.502
904	29	38	0.470
905	29	39	0.442
906	29	40	0.416
907	29	49	0.967
908	29	50	0.863
909	29	51	0.777
910	29	52	0.705
911	29	53	0.644
912	29	54	0.591
913	29	55	0.545
914	29	56	0.504
915	29	57	0.468
916	29	58	0.436
917	29	59	0.408
918	29	60	0.382
919	30	30	1.000
920	30	31	0.904
921	30	32	0.824
922	30	33	0.755
923	30	34	0.697
924	30	35	0.646
925	30	36	0.601
926	30	37	0.561
927	30	38	0.525

Table A1. *Cont.*

Pounding Case	Building 1	Building 2	Period Ratio
928	30	39	0.493
929	30	40	0.464
930	30	50	0.963
931	30	51	0.868
932	30	52	0.787
933	30	53	0.719
934	30	54	0.660
935	30	55	0.609
936	30	56	0.563
937	30	57	0.523
938	30	58	0.487
939	30	59	0.455
940	30	60	0.426
941	31	31	1.000
942	31	32	0.912
943	31	33	0.836
944	31	34	0.771
945	31	35	0.714
946	31	36	0.664
947	31	37	0.620
948	31	38	0.581
949	31	39	0.545
950	31	40	0.514
951	31	51	0.960
952	31	52	0.871
953	31	53	0.795
954	31	54	0.730
955	31	55	0.673
956	31	56	0.623
957	31	57	0.579
958	31	58	0.539
959	31	59	0.504
960	31	60	0.472
961	32	32	1.000
962	32	33	0.917
963	32	34	0.846
964	32	35	0.783
965	32	36	0.729
966	32	37	0.680
967	32	38	0.637
968	32	39	0.598

Table A1. *Cont.*

Pounding Case	Building 1	Building 2	Period Ratio
969	32	40	0.563
970	32	52	0.956
971	32	53	0.872
972	32	54	0.801
973	32	55	0.738
974	32	56	0.684
975	32	57	0.635
976	32	58	0.591
977	32	59	0.553
978	32	60	0.517
979	33	33	1.000
980	33	34	0.922
981	33	35	0.855
982	33	36	0.795
983	33	37	0.742
984	33	38	0.695
985	33	39	0.653
986	33	40	0.615
987	33	53	0.951
988	33	54	0.873
989	33	55	0.805
990	33	56	0.746
991	33	57	0.692
992	33	58	0.645
993	33	59	0.603
994	33	60	0.564
995	34	34	1.000
996	34	35	0.926
997	34	36	0.862
998	34	37	0.804
999	34	38	0.753
1000	34	39	0.708
1001	34	40	0.666
1002	34	54	0.947
1003	34	55	0.873
1004	34	56	0.808
1005	34	57	0.751
1006	34	58	0.699
1007	34	59	0.653
1008	34	60	0.612
1009	35	35	1.000

Table A1. *Cont.*

Pounding Case	Building 1	Building 2	Period Ratio
1010	35	36	0.930
1011	35	37	0.868
1012	35	38	0.813
1013	35	39	0.764
1014	35	40	0.719
1015	35	55	0.943
1016	35	56	0.872
1017	35	57	0.810
1018	35	58	0.755
1019	35	59	0.705
1020	35	60	0.660
1021	36	36	1.000
1022	36	37	0.934
1023	36	38	0.874
1024	36	39	0.821
1025	36	40	0.773
1026	36	56	0.938
1027	36	57	0.871
1028	36	58	0.811
1029	36	59	0.758
1030	36	60	0.710
1031	37	37	1.000
1032	37	38	0.937
1033	37	39	0.880
1034	37	40	0.828
1035	37	57	0.933
1036	37	58	0.869
1037	37	59	0.812
1038	37	60	0.760
1039	38	38	1.000
1040	38	39	0.939
1041	38	40	0.884
1042	38	58	0.928
1043	38	59	0.867
1044	38	60	0.812
1045	39	39	1.000
1046	39	40	0.942
1047	39	59	0.923
1048	39	60	0.865
1049	40	40	1.000
1050	40	60	0.918

Table A1. *Cont.*

Pounding Case	Building 1	Building 2	Period Ratio
1051	41	41	1.000
1052	41	42	0.543
1053	41	43	0.366
1054	41	44	0.275
1055	41	45	0.219
1056	41	46	0.182
1057	41	47	0.155
1058	41	48	0.135
1059	41	49	0.119
1060	41	50	0.106
1061	41	51	0.096
1062	41	52	0.087
1063	41	53	0.079
1064	41	54	0.073
1065	41	55	0.067
1066	41	56	0.062
1067	41	57	0.058
1068	41	58	0.054
1069	41	59	0.050
1070	41	60	0.047
1071	42	42	1.000
1072	42	43	0.675
1073	42	44	0.506
1074	42	45	0.404
1075	42	46	0.335
1076	42	47	0.286
1077	42	48	0.248
1078	42	49	0.219
1079	42	50	0.195
1080	42	51	0.176
1081	42	52	0.160
1082	42	53	0.146
1083	42	54	0.134
1084	42	55	0.123
1085	42	56	0.114
1086	42	57	0.106
1087	42	58	0.099
1088	42	59	0.092
1089	42	60	0.087
1090	43	43	1.000
1091	43	44	0.750

Table A1. *Cont.*

Pounding Case	Building 1	Building 2	Period Ratio
1092	43	45	0.599
1093	43	46	0.497
1094	43	47	0.424
1095	43	48	0.368
1096	43	49	0.325
1097	43	50	0.290
1098	43	51	0.261
1099	43	52	0.237
1100	43	53	0.216
1101	43	54	0.198
1102	43	55	0.183
1103	43	56	0.169
1104	43	57	0.157
1105	43	58	0.147
1106	43	59	0.137
1107	43	60	0.128
1108	44	44	1.000
1109	44	45	0.798
1110	44	46	0.663
1111	44	47	0.565
1112	44	48	0.491
1113	44	49	0.433
1114	44	50	0.386
1115	44	51	0.348
1116	44	52	0.316
1117	44	53	0.288
1118	44	54	0.264
1119	44	55	0.244
1120	44	56	0.226
1121	44	57	0.210
1122	44	58	0.195
1123	44	59	0.182
1124	44	60	0.171
1125	45	45	1.000
1126	45	46	0.830
1127	45	47	0.707
1128	45	48	0.615
1129	45	49	0.542
1130	45	50	0.484
1131	45	51	0.435
1132	45	52	0.395

Table A1. *Cont.*

Pounding Case	Building 1	Building 2	Period Ratio
1133	45	53	0.361
1134	45	54	0.331
1135	45	55	0.305
1136	45	56	0.283
1137	45	57	0.263
1138	45	58	0.245
1139	45	59	0.229
1140	45	60	0.214
1141	46	46	1.000
1142	46	47	0.852
1143	46	48	0.741
1144	46	49	0.653
1145	46	50	0.583
1146	46	51	0.525
1147	46	52	0.476
1148	46	53	0.435
1149	46	54	0.399
1150	46	55	0.368
1151	46	56	0.341
1152	46	57	0.316
1153	46	58	0.295
1154	46	59	0.275
1155	46	60	0.258
1156	47	47	1.000
1157	47	48	0.869
1158	47	49	0.766
1159	47	50	0.684
1160	47	51	0.616
1161	47	52	0.559
1162	47	53	0.510
1163	47	54	0.468
1164	47	55	0.432
1165	47	56	0.400
1166	47	57	0.371
1167	47	58	0.346
1168	47	59	0.323
1169	47	60	0.303
1170	48	48	1.000
1171	48	49	0.882
1172	48	50	0.787
1173	48	51	0.709

Table A1. *Cont.*

Pounding Case	Building 1	Building 2	Period Ratio
1174	48	52	0.643
1175	48	53	0.587
1176	48	54	0.539
1177	48	55	0.497
1178	48	56	0.460
1179	48	57	0.427
1180	48	58	0.398
1181	48	59	0.372
1182	48	60	0.348
1183	49	49	1.000
1184	49	50	0.892
1185	49	51	0.804
1186	49	52	0.729
1187	49	53	0.666
1188	49	54	0.611
1189	49	55	0.564
1190	49	56	0.522
1191	49	57	0.485
1192	49	58	0.451
1193	49	59	0.422
1194	49	60	0.395
1195	50	50	1.000
1196	50	51	0.901
1197	50	52	0.817
1198	50	53	0.746
1199	50	54	0.685
1200	50	55	0.632
1201	50	56	0.585
1202	50	57	0.543
1203	50	58	0.506
1204	50	59	0.473
1205	50	60	0.443
1206	51	51	1.000
1207	51	52	0.908
1208	51	53	0.828
1209	51	54	0.761
1210	51	55	0.701
1211	51	56	0.649
1212	51	57	0.603
1213	51	58	0.562
1214	51	59	0.525

Table A1. *Cont.*

Pounding Case	Building 1	Building 2	Period Ratio
1215	51	60	0.491
1216	52	52	1.000
1217	52	53	0.913
1218	52	54	0.838
1219	52	55	0.773
1220	52	56	0.715
1221	52	57	0.664
1222	52	58	0.619
1223	52	59	0.578
1224	52	60	0.541
1225	53	53	1.000
1226	53	54	0.918
1227	53	55	0.847
1228	53	56	0.784
1229	53	57	0.728
1230	53	58	0.678
1231	53	59	0.633
1232	53	60	0.593
1233	54	54	1.000
1234	54	55	0.922
1235	54	56	0.854
1236	54	57	0.793
1237	54	58	0.738
1238	54	59	0.690
1239	54	60	0.646
1240	55	55	1.000
1241	55	56	0.926
1242	55	57	0.860
1243	55	58	0.801
1244	55	59	0.748
1245	55	60	0.701
1246	56	56	1.000
1247	56	57	0.929
1248	56	58	0.865
1249	56	59	0.808
1250	56	60	0.757
1251	57	57	1.000
1252	57	58	0.932
1253	57	59	0.870
1254	57	60	0.815
1255	58	58	1.000

Table A1. *Cont.*

Pounding Case	Building 1	Building 2	Period Ratio
1256	58	59	0.934
1257	58	60	0.875
1258	59	59	1.000
1259	59	60	0.936
1260	60	60	1.000

References

1. Anagnostopoulos, S.A. Pounding of buildings in series during earthquakes. *Earthq. Eng. Struct. Dyn.* **1988**, *16*, 443–456. [CrossRef]
2. Favvata, M.J. Minimum required separation gap for adjacent RC frames with potential inter-story seismic pounding. *Eng. Struct.* **2017**, *152*, 643–659. [CrossRef]
3. Mavronicola, E.A.; Polycarpou, P.C.; Komodromos, P. Effect of ground motion directionality on the seismic response of base isolated buildings pounding against adjacent structures. *Eng. Struct.* **2020**, *207*, 110202. [CrossRef]
4. Miari, M.; Jankowski, R. Pounding between high-rise buildings with different structural arrangements. In Proceedings of the International Conference on Wave Mechanics and Vibrations, Lisbon, Portugal, 4–6 July 2022; pp. 807–816.
5. Miari, M.; Jankowski, R. Incremental dynamic analysis and fragility assessment of buildings with different structural arrangements experiencing earthquake-induced structural pounding. In Proceedings of the International Conference on Computational Science, London, UK, 21–23 June 2022; pp. 117–124.
6. Rosenblueth, E.; Meli, R. The 1985 Mexico earthquake. *Concr. Int.* **1986**, *8*, 23–34.
7. Anagnostopoulos, S. Building pounding re-examined: How serious a problem is it. In Proceedings of the Eleventh World Conference on Earthquake Engineering, Acapulco, Mexico, 23–28 June 1996; Pergamon: Oxford, UK, 1996; p. 2108.
8. Kasai, K.; Maison, B.F. Building pounding damage during the 1989 Loma Prieta earthquake. *Eng. Struct.* **1997**, *19*, 195–207. [CrossRef]
9. Romão, X.; Costa, A.; Paupério, E.; Rodrigues, H.; Vicente, R.; Varum, H.; Costa, A. Field observations and interpretation of the structural performance of constructions after the 11 May 2011 Lorca earthquake. *Eng. Fail. Anal.* **2013**, *34*, 670–692. [CrossRef]
10. Wibowo, A.; Kafle, B.; Kermani, A.M.; Lam, N.T.; Wilson, J.L.; Gad, E.F. Damage in the 2008 China earthquake. In Proceedings of the Australian Earthquake Engineering Society Conference, Ballarat, Australia, 21–23 November 2008; pp. 1–8.
11. Cole, G.; Dhakal, R.; Carr, A.; Bull, D. Interbuilding pounding damage observed in the 2010 Darfield earthquake. *Bull. N. Z. Soc. Earthq. Eng.* **2010**, *43*, 382–386. [CrossRef]
12. Cole, G.; Dhakal, R.; Carr, A.; Bull, D. Case studies of observed pounding damage during the 2010 Darfield earthquake. In Proceedings of the 9th Pacific Conference on Earthquake Engineering, Auckland, The Netherlands, 14–16 April 2011.
13. Cole, G.; Dhakal, R.; Chouw, N. Building Pounding Damage Observed in the 2011 Christchurch earthquake Christchurch Earthquake. In Proceedings of the 15th World Conference on Earthquake Engineering, Lisbon, Portugal, 24–28 September 2012.
14. Cole, G.L.; Dhakal, R.P.; Turner, F.M. Building pounding damage observed in the 2011 Christchurch earthquake. *Earthq. Eng. Struct. Dyn.* **2012**, *41*, 893–913. [CrossRef]
15. Gautam, D.; Rodrigues, H.; Bhetwal, K.K.; Neupane, P.; Sanada, Y. Common structural and construction deficiencies of Nepalese buildings. *Innov. Infrastruct. Solut.* **2016**, *1*, 1. [CrossRef]
16. Sharma, K.; Deng, L.; Noguez, C.C. Field investigation on the performance of building structures during the April 25, 2015, Gorkha earthquake in Nepal. *Eng. Struct.* **2016**, *121*, 61–74. [CrossRef]
17. Gautam, D.; Chaulagain, H. Structural performance and associated lessons to be learned from world earthquakes in Nepal after 25 April 2015 (MW 7.8) Gorkha earthquake. *Eng. Fail. Anal.* **2016**, *68*, 222–243. [CrossRef]
18. Shakya, K.; Pant, D.; Maharjan, M.; Bhagat, S.; Wijeyewickrema, A.; Maskey, P. Lessons learned from performance of buildings during the September 18, 2011 earthquake in Nepal. *Asian J. Civ. Eng. (Build. Hous.)* **2013**, *14*, 719–733.
19. Rai, D.C.; Singhal, V.; Raj, S.B.; Sagar, S.L. Reconnaissance of the effects of the M7. 8 Gorkha (Nepal) earthquake of April 25, 2015. *Geomat. Nat. Hazards Risk* **2016**, *7*, 1–17. [CrossRef]
20. Shrestha, B.; Hao, H. Building pounding damages observed during the 2015 Gorkha earthquake. *J. Perform. Constr. Facil.* **2018**, *32*, 04018006. [CrossRef]
21. Miari, M.; Choong, K.K.; Jankowski, R. Seismic pounding between adjacent buildings: Identification of parameters, soil interaction issues and mitigation measures. *Soil Dyn. Earthq. Eng.* **2019**, *121*, 135–150. [CrossRef]
22. Miari, M.; Choong, K.K.; Jankowski, R. Seismic pounding between bridge segments: A state-of-the-art review. *Arch. Comput. Methods Eng.* **2021**, *28*, 495–504. [CrossRef]
23. Raheem, S.E.A. Seismic pounding between adjacent building structures. *Electron. J. Struct. Eng.* **2006**, *6*, 155.
24. Rojas, F.R.; Anderson, J.C. Pounding of an 18-story building during recorded earthquakes. *J. Struct. Eng.* **2012**, *138*, 1530–1544. [CrossRef]

25. Raheem, S.E.A. Mitigation measures for earthquake induced pounding effects on seismic performance of adjacent buildings. *Bull. Earthq. Eng.* **2014**, *12*, 1705–1724. [CrossRef]
26. Inel, M.; Cayci, B.T.; Kamal, M.; Altinel, O. Structural Pounding of Mid-Rise RC Buildings during Earthquakes. In Proceedings of the 3rd European Conference on Earthquake Engineering and Seismology, Bucharest, Romania, 4–9 September 2022.
27. Efraimiadou, S.; Hatzigeorgiou, G.D.; Beskos, D.E. Structural pounding between adjacent buildings subjected to strong ground motions. Part I: The effect of different structures arrangement. *Earthq. Eng. Struct. Dyn.* **2013**, *42*, 1509–1528. [CrossRef]
28. Jameel, M.; Islam, A.; Hussain, R.R.; Hasan, S.D.; Khaleel, M. Non-linear FEM analysis of seismic induced pounding between neighbouring multi-storey structures. *Lat. Am. J. Solids Struct.* **2013**, *10*, 921–939. [CrossRef]
29. Anagnostopoulos, S.A.; Spiliopoulos, K.V. An investigation of earthquake induced pounding between adjacent buildings. *Earthq. Eng. Struct. Dyn.* **1992**, *21*, 289–302. [CrossRef]
30. Jaradat, Y.; Far, H.; Mortazavi, M. Experimental evaluation of theoretical impact models for seismic pounding. *J. Earthq. Eng.* 2022. [CrossRef]
31. Maison, B.F.; Kasai, K. Dynamics of pounding when two buildings collide. *Earthq. Eng. Struct. Dyn.* **1992**, *21*, 771–786. [CrossRef]
32. Mouzakis, H.P.; Papadrakakis, M. Three dimensional nonlinear building pounding with friction during earthquakes. *J. Earthq. Eng.* **2004**, *8*, 107–132. [CrossRef]
33. Gong, L.; Hao, H. Analysis of coupled lateral-torsional-pounding responses of one-storey asymmetric adjacent structures subjected to bi-directional ground motions Part I: Uniform ground motion input. *Adv. Struct. Eng.* **2005**, *8*, 463–479. [CrossRef]
34. Crozet, V.; Politopoulos, I.; Yang, M.; Martinez, J.M.; Erlicher, S. Sensitivity analysis of pounding between adjacent structures. *Earthq. Eng. Struct. Dyn.* **2018**, *47*, 219–235. [CrossRef]
35. Crozet, V.; Politopoulos, I.; Yang, M.; Martinez, J.; Erlicher, S. Influential structural parameters of pounding between buildings during earthquakes. *Procedia Eng.* **2017**, *199*, 1092–1097. [CrossRef]
36. *UBC97*; Uniform Building Code. International Conference of Building Officials: Whittier, CA, USA, 1997.
37. Jeng, V.; Kasai, K.; Maison, B.F. A spectral difference method to estimate building separations to avoid pounding. *Earthq. Spectra* **1992**, *8*, 201–223. [CrossRef]
38. *AS 1170.4—2007*; Structural Design Actions: Earthquake Actions in Australia. Standards Australia: Sydney, NSW, Australia, 2007.
39. Naderpour, H.; Khatami, S.M.; Barros, R.C. Prediction of critical distance between two MDOF systems subjected to seismic excitation in terms of artificial neural networks. *Period. Polytech. Civ. Eng.* **2017**, *61*, 516–529. [CrossRef]
40. Stewart, J.P.; Fenves, G.L.; Seed, R.B. Seismic soil-structure interaction in buildings. I: Analytical methods. *J. Geotech. Geoenviron. Eng.* **1999**, *125*, 26–37. [CrossRef]
41. Tabatabaiefar, H.R.; Clifton, T. Significance of considering soil-structure interaction effects on seismic design of unbraced building frames resting on soft soils. *Aust. Geomech. J.* **2016**, *51*, 55–64.
42. Far, H. Dynamic behaviour of unbraced steel frames resting on soft ground. *Steel Constr.* **2019**, *12*, 135–140. [CrossRef]
43. Tabatabaiefar, S.H.R.; Fatahi, B.; Samali, B. Finite difference modelling of soil-structure interaction for seismic design of moment resisting building frames. *Aust. Geomech. J.* **2012**, *47*, 113–120.
44. Tabatabaiefar, H.R.; Fatahi, B.; Samali, B. Effects of dynamic soil-structure interaction on performance level of moment resisting buildings resting on different types of soil. In Proceedings of the 2011 Pacific Conference on Earthquake Engineering (PCEE), Auckland, New Zealand, 14–16 April 2011.
45. Hamid Reza Tabatabaiefar, S.; Fatahi, B.; Samali, B. An empirical relationship to determine lateral seismic response of mid-rise building frames under influence of soil–structure interaction. *Struct. Des. Tall Spec. Build.* **2014**, *23*, 526–548. [CrossRef]
46. Tabatabaiefar, H.R.; Fatahi, B.; Ghabraie, K.; Zhou, W.-H. Evaluation of numerical procedures to determine seismic response of structures under influence of soil-structure interaction. *Struct. Eng. Mech.* **2015**, *56*, 27–47. [CrossRef]
47. Wang, L.; Shi, W.; Zhou, Y. Adaptive-passive tuned mass damper for structural aseismic protection including soil–structure interaction. *Soil Dyn. Earthq. Eng.* **2022**, *158*, 107298. [CrossRef]
48. Wang, L.; Nagarajaiah, S.; Zhou, Y.; Shi, W. Experimental study on adaptive-passive tuned mass damper with variable stiffness for vertical human-induced vibration control. *Eng. Struct.* **2023**, *280*, 115714. [CrossRef]
49. Wang, L.; Nagarajaiah, S.; Shi, W.; Zhou, Y. Seismic performance improvement of base-isolated structures using a semi-active tuned mass damper. *Eng. Struct.* **2022**, *271*, 114963. [CrossRef]
50. Tabatabaiefar, H.R.; Massumi, A. A simplified method to determine seismic responses of reinforced concrete moment resisting building frames under influence of soil–structure interaction. *Soil Dyn. Earthq. Eng.* **2010**, *30*, 1259–1267. [CrossRef]
51. Tabatabaiefar, H.R.; Fatahi, B. Idealisation of soil–structure system to determine inelastic seismic response of mid-rise building frames. *Soil Dyn. Earthq. Eng.* **2014**, *66*, 339–351. [CrossRef]
52. Tabatabaiefar, H.R. Detail design and construction procedure of laminar soil containers for experimental shaking table tests. *Int. J. Geotech. Eng.* **2016**, *10*, 328–336. [CrossRef]
53. Tabatabaiefar, S.H.R.; Fatahi, B.; Samali, B. Numerical and experimental investigations on seismic response of building frames under influence of soil-structure interaction. *Adv. Struct. Eng.* **2014**, *17*, 109–130. [CrossRef]
54. Tabatabaiefar, H.R.; Mansoury, B. Detail design, building and commissioning of tall building structural models for experimental shaking table tests. *Struct. Des. Tall Spec. Build.* **2016**, *25*, 357–374. [CrossRef]
55. Tabatabaiefar, H.R. Development of synthetic soil mixture for experimental shaking table tests on building frames resting on soft soils. *Geomech. Geoengin.* **2017**, *12*, 28–35. [CrossRef]

56. Naserkhaki, S.; El-Rich, M.; Aziz, F.; Pourmohammad, H. Pounding between adjacent buildings of varying height coupled through soil. *Struct. Eng. Mech.* **2014**, *52*, 573–593. [CrossRef]
57. Fatahi, B.; Van Nguyen, Q.; Xu, R.; Sun, W.-j. Three-dimensional response of neighboring buildings sitting on pile foundations to seismic pounding. *Int. J. Geomech.* **2018**, *18*, 04018007. [CrossRef]
58. Ghandil, M.; Aldaikh, H. Damage-based seismic planar pounding analysis of adjacent symmetric buildings considering inelastic structure–soil–structure interaction. *Earthq. Eng. Struct. Dyn.* **2017**, *46*, 1141–1159. [CrossRef]
59. Naserkhaki, S.; Aziz, F.N.; Pourmohammad, H. Earthquake induced pounding between adjacent buildings considering soil-structure interaction. *Earthq. Eng. Eng. Vib.* **2012**, *11*, 343–358. [CrossRef]
60. Farghaly, A.A. Seismic analysis of adjacent buildings subjected to double pounding considering soil–structure interaction. *Int. J. Adv. Struct. Eng.* **2017**, *9*, 51–62. [CrossRef]
61. Kontoni, D.-P.N.; Farghaly, A.A. Seismic response of adjacent unequal buildings subjected to double pounding considering soil-structure interaction. *Computation* **2018**, *6*, 10. [CrossRef]
62. Naserkhaki, S.; El Rich, M.; Abdul, A.F.; Pourmohammad, H. Separation gap, a critical factor in earthquake induced pounding between adjacent buildings. *Asian J. Civ. Eng. (Build. Hous.)* **2013**, *14*, 881–898.
63. Li, P.; Liu, S.; Lu, Z. Studies on pounding response considering structure-soil-structure interaction under seismic loads. *Sustainability* **2017**, *9*, 2219. [CrossRef]
64. Shakya, K.; Wijeyewickrema, A.C. Mid-column pounding of multi-story reinforced concrete buildings considering soil effects. *Adv. Struct. Eng.* **2009**, *12*, 71–85. [CrossRef]
65. Shakya, K.; Wijeyewickrema, A.C.; Ohmachi, T. Mid-column seismic pounding of reinforced concrete buildings in a row considering effects of soil. In Proceedings of the 14th World Conference on Earthquake Engineering, Beijing, China, 12–17 October 2008; pp. 12–17.
66. Miari, M.; Jankowski, R. Analysis of pounding between adjacent buildings founded on different soil types. *Soil Dyn. Earthq. Eng.* **2022**, *154*, 107156. [CrossRef]
67. Miari, M.; Jankowski, R. Incremental dynamic analysis and fragility assessment of buildings founded on different soil types experiencing structural pounding during earthquakes. *Eng. Struct.* **2022**, *252*, 113118. [CrossRef]
68. Miari, M.; Jankowski, R. Pounding between high-rise buildings founded on different soil types. In Proceedings of the 17th World Conference on Earthquake Engineering, Sendai, Japan, 27 September 2021.
69. *ASCE Standard ASCE/SEI 7-10*; Minimum Design Loads for Buildings and Other Structures. American Society of Civil Engineers: Reston, VA, USA, 2013.
70. Miari, M.; Jankowski, R. Analysis of floor-to-column pounding of buildings founded on different soil types. *Bull. Earthq. Eng.* **2022**, *20*, 7241–7262. [CrossRef]
71. Miari, M.; Jankowski, R. Shaking table experimental study on pounding between adjacent structures founded on different soil types. *Structures* **2022**, *44*, 851–879. [CrossRef]
72. Miari, M.; Jankowski, R. Seismic gap between buildings founded on different soil types experiencing pounding during earthquakes. *Earthq. Spectra* **2022**, *38*, 2183–2206. [CrossRef]
73. Miari, M.; Jankowski, R. Analysis of the effect of the seismic gap on the response of buildings experiencing pounding during earthquakes. *AIP Conf. Proc.* **2023**, *2848*, 020021.
74. Miari, M.; Jankowski, R. Assessment of codes recommendations for the evaluation of the seismic gap of buildings founded on different soil types. *AIP Conf. Proc.* **2023**, *2848*, 020022.
75. Yaghmaei-Sabegh, S.; Jalali-Milani, N. Pounding force response spectrum for near-field and far-field earthquakes. *Sci. Iran.* **2012**, *19*, 1236–1250. [CrossRef]
76. Jaradat, Y.; Far, H.; Saleh, A. Examining the adequacy of separation gaps between adjacent buildings under near-field and far-field earthquakes. *WIT Trans. Built Environ.* **2021**, *202*, 59–71.
77. Bathe, K.-J.; Wilson, E.L. *Numerical Methods in Finite Element Analysis*; Prentice Hall: Hoboken, NJ, USA, 1976.
78. Hao, H. Analysis of seismic pounding between adjacent buildings. *Aust. J. Struct. Eng.* **2015**, *16*, 208–225. [CrossRef]
79. Pacific Earthquake Engineering Research Centre (PEER NGA DATABASE). Available online: https://ngawest2.berkeley.edu/ (accessed on 8 August 2023).
80. *ETABS*, version 18; Computers & Structures Inc.: Berkeley, CA, USA, 2018.
81. DesRoches, R.; Muthukumar, S. Effect of pounding and restrainers on seismic response of multiple-frame bridges. *J. Struct. Eng.* **2002**, *128*, 860–869. [CrossRef]
82. Bendat, J.; Piersol, A. *Random Data: Analysis and Measurement Procedures*; Wiley-Intersci: New York, NY, USA, 1971; Volume 1, p. 75.
83. Ibrahimbegovic, A.; Wilson, E.L. Simple numerical algorithms for the mode superposition analysis of linear structural systems with non-proportional damping. *Comput. Struct.* **1989**, *33*, 523–531. [CrossRef]
84. Jaradat, Y.; Far, H. Optimum stiffness values for impact element models to determine pounding forces between adjacent buildings. *Struct. Eng. Mech.* **2020**, *77*, 293–304.